

**Cardiac and peripheral hemodynamic effects of selective endothelin-A
receptor antagonism**

Edgár Eszlári MD

Ph.D. Thesis

**Institute of Surgical Research and Department of Cardiac Surgery
University of Szeged, Hungary**

2011

Szeged

List of full papers related to the subject of the thesis

1. Szabó A, Suki B, Csonka E, **Eszlári E**, Kucsá K, Vajda K, Kaszaki J, Boros M: Flowmotion in the intestinal villi during hemorrhagic shock. A new method to characterize the microcirculatory changes. *Shock* 21:320-329, 2004. IF 3.122
2. **Eszlári E**, Czóbel M, Molnár G, Bogáts G, Kaszaki J, Nagy S, Boros M: Modulation of cardiac contractility through endothelin-1 release and myocardial mast cell degranulation. *Acta Physiol Hun* 95:301-319, 2008. IF 0.491
3. Molnár G, **Eszlári E**, Czóbel M, Kaszaki J, Bogáts G, Nagy S, Boros M: A nitrogén-monoxid-szintézis gátlása endothelinfüggő szívkontraktilitás növekedéshez vezet. *Cardiologica Hungarica* 40(1):1-6, 2010. IF 0.0

List of abstracts related to the subject of the thesis

1. Kaszaki J, Molnár G, **Eszlári E**, Csonka E, Nagy S, Petri I, Boros M: The role of mast cells and endothelin-1 in the circulatory effects of colloid-crystalloid resuscitation fluids. *European Surgical Research* 33 (Suppl. 1): 155, 2001.
2. **Eszlári E**, Csonka E, Kaszaki J, Molnár G, Szabó A, Boros M: Comparison of the circulatory effects of different hypertonic colloid volume expanders. *European Surgical Research* 34 (Suppl. 1): 91, 2002.
3. **Eszlári E**, Csonka E, Kaszaki J, Szabó A, Nagy S, Boros M: Hypertonic colloid volume expanders differentially affect cardiac contractility. *Shock* 18 (Suppl.): 6-7, 2002.
4. **Eszlári E**, Csonka E, Kaszaki J, Nagy S, Bogáts G, Boros M: Hypertonic dextran volume expanders with different molecular weights differentially affect cardiac contractility. *Experimental and Clinical Cardiology* 8:38, 2003.
5. Kaszaki J, Czóbel M, **Eszlári E**, Csonka E, Nagy S, Boros M: Interaction between endothelin and nitric oxide in regulation of cardiac contractility. A possible role of cardiac mast cells. *Experimental and Clinical Cardiology* 8:42-43, 2003.
6. Kaszaki J, **Eszlári E**, Csonka E, Czóbel M, Nagy S, Boros M: Endothelin-dependent changes in cardiac contractility after hypertonic colloid infusions. The role of mast cells. *Shock* 21 (Suppl.): 96, 2004.

CONTENTS

List of papers related to the subject of the thesis	2
List of abbreviations	4
1. Introduction	5
1.1. Regulation of cardiac performance	5
1.2. Analysis of cardiac function	6
1.3. Characteristics of microcirculation	8
1.4. Analysis of microhemodynamics	9
1.5. The vascular endothelium	10
1.6. Vasoregulatory role of endothelins	11
1.7. The ETR-p1/fl peptide	13
1.8. Significance of fluid resuscitation in circulatory disturbances	14
2. Main goals	15
3. Materials and Methods	17
3.1. Surgical preparation	17
3.2. Macrohemodynamic measurements	18
3.3. Microcirculatory measurements in Study III	18
3.4. Biochemical measurements	19
3.5. Experimental protocols	20
3.6. Statistical analysis	21
4. Results	22
4.1. Study I: Cardiac and peripheral effects of hypertonic saline - dextran treatment	22
4.2. Study II: Cardiac effects of decreased NO production	26
4.3. Study III: Effects of hypertonic saline - dextran and endothelin-A receptor antagonist treatments in hemorrhagic shock	28
5. Discussion	33
6. Summary of new findings	40
7. Acknowledgments	41
8. References	42
9. Annex	50

List of abbreviations

CI	-	cardiac index
cNOS	-	Ca ²⁺ -dependent constitutive nitric oxide synthase
CO	-	cardiac output
CVP	-	central venous pressure
ECE	-	ET converting enzyme
ESPVR	-	end-systolic pressure-volume relationship
ET	-	endothelin
ET-A	-	endothelin-A receptor
ET-B	-	endothelin-B receptor
FCD	-	functional capillary density
FFR	-	force-frequency relation
HR	-	heart rate
HS	-	hemorrhagic shock
HSD	-	hypertonic saline – dextran
iNOS	-	Ca ²⁺ -independent inducible nitric oxide synthase
IVM	-	intravital microscopy (and computer-assisted image analysis system)
LVD	-	left ventricular diameter
LVP	-	left ventricular pressure
MAP	-	mean arterial pressure
MPO	-	myeloperoxidase
NNA	-	N-ω-nitro-L-arginine
NO	-	nitric oxide
OPS	-	Orthogonal Polarization Spectral imaging
PiCCO	-	Pulse Contour Cardiac Output monitor
PMNs	-	polymorphonuclear leukocytes
PRSW	-	preload recruitable stroke work
QO ₂	-	oxygen delivery
RBCV	-	red blood cell velocity
ROS	-	reactive oxygen species
SV	-	stroke volume
TPR	-	total peripheral vascular resistance
VO ₂	-	oxygen consumption

1. Introduction

The endothelins (ETs) are powerful vasoactive peptides, of which ET-1 is the major isoform. There is a substantial and growing body of evidence that ET-1 and the activation of ET receptors play decisive roles both in physiological vasoregulation and during acute disorders of the cardiovascular system. The peptide ET-1 was originally described as the most potent vasoconstrictor agent produced by endothelial cells (Yanagisawa 1988). Nevertheless, it has been established that other cells, such as leukocytes, macrophages, smooth muscle cells and cardiomyocytes, can also be sources of ET-1 release in pathophysiological circulatory states. It has further been demonstrated that plasma ET-1 levels correlate linearly with the severity of circulatory disorders; accordingly, the possibility of ET receptor antagonist therapies has received increasing attention. Given this background, the general aim of our studies was to examine and characterize the consequences of ET receptor antagonism on central and peripheral hemodynamics, and on macro- and microcirculatory patterns in healthy controls and in conditions potentially associated with ET-1 overproduction.

1.1. Regulation of cardiac performance

The cardiac pump function or performance depends on many parameters, which act in parallel, and synergy normally exists to some degree. Examples of performance parameters include cardiac output (CO), stroke volume (SV), rate of fiber shortening, stroke work, myocardial compliance and ejection fraction. Myocardial performance is dependent on *preload*, *afterload*, *heart rate (HR)* and *contractility*, and is influenced by neurohormonal and local endothelial-derived factors. The main characteristics of the major performance parameters are summarized as follows.

1. The *preload* is a result of heterometric autoregulation, Starling's law of the heart. When the cardiac muscle is stretched, it tends to develop greater contractile tension on excitation. Thus, stroke volume tends to increase in proportion to preload (diastolic filling).
2. The *afterload* is determined by the total peripheral vascular resistance. A sudden rise in afterload causes an immediate decrease in ejection fraction and a rise in end-systolic volume. The compensation can occur in two ways. An increased end-systolic volume coupled with a normal venous return leads to an elevated preload, and the SV is maintained by Starling's law. In addition, contractility may increase secondary to an increased coronary perfusion pressure, the Gregg effect (Anrep 1933, Gregg 1963). Thus, small changes in afterload have a minimal steady - state effect on performance as measured by SV or CO despite, a significant initial effect.

3. *HR* increases are usually associated with small increases in contractile force (see below). However, an increased *HR* is associated with a proportionally shorter diastolic filling time and for this reason the atrial contraction becomes far more important at high *HR*s. It has been established that the heart contractility depends on increasing *HR* in most mammals. The ventricular myocardium has an inherent ability to increase its strength of contraction, independently of neurohormonal control, in response to an increase in contraction. In humans, this myocardial property causes the contractile force to rise, as the contraction frequency is increased from 60 to about 180-200 beats per minute and then to decline with further increase in frequency (the force-frequency relation; *FFR*).

4. *Contractility* is often defined as the intrinsic ability of a cardiac muscle fiber to contract at a given fiber length. Changes in the ability to produce force during contraction result from different degrees of binding between myosin and actin filaments. The degree of binding that occurs depends on the concentration of Ca^{2+} in the cell. The cytosolic Ca^{2+} level is the determinant of the involved myocardial fiber number in the contraction process and the maximal velocity of myocardial fiber shortening. An increased contractility - positive inotropic effect is reflected in a higher myocardial fiber shortening velocity with a higher cytosolic Ca^{2+} concentration in systole: more troponin is activated from higher levels of Ca^{2+} with more actin-myosin cross-bridges in unit time, and ultimately the myocardial fiber contraction is more extensive and faster. The performance improves at any given preload and afterload.

Neural influences mean that the sympathetic discharge to the ventricles increases their contractility. Likewise, circulating epinephrine increases contractility. Other inotropic agents, such as Ca^{2+} sensitizers, phosphodiesterase inhibitors, cardiac glycosides, catecholamines and endothelial derived factors, also modify the myocardial contractility and/or Ca^{2+} availability.

1.2. Analysis of cardiac function

As many of the indices of myocardial performance are independent, qualifying the contribution of each component to the overall cardiac function is not possible at present, and the clinical utility of monitoring each individually is not therefore established. Bedside measurements of left ventricular (*LV*) dimensions, volumes and ejection fraction and the other indices of systolic and diastolic function can now be carried out, but their routine use in clinical practice remains unproven. Transthoracic or transesophageal echography has an important and established diagnostic role and has been used successfully to monitor segmental wall motion, and ejection fraction, to measure cardiac cavities, valvular function, *etc.*, but practical considerations seriously limit its potential for routine use and it is not able

to measure CO continuously. Radionuclide techniques allow the measurement of many of the same parameters and have the potential for continuous use, but practical problems and the additional risk of radiation exposure may limit their application in the critical care environment. Doppler techniques are noninvasive, provide continuous data and are simple to operate, but the data provided have important limitations.

In clinical practice, there are two prevalent invasive techniques, which can measure and calculate preload and CO parameters with the application of thermodilution method. One of these techniques applies the pulmonary artery (Swan-Ganz) catheter, which has been used for over 20 years. Questions remain regarding the information it provides concerning the myocardial function, and the extent to which it should influence therapeutic decisions is still controversial. However, with the development of additional facilities, and particularly the continuous measurement of CO, the pulmonary artery catheter remains the mainstay in the bedside monitoring of myocardial performance in critically ill patients. Another invasive technique is the “Pulse Contour Cardiac Output” (PiCCO) system, which uses volumetric, transpulmonary thermodilution. The main advantages of the PiCCO system are the online function and the possibility for pulse contour analysis.

Examinations of cardiac contractility in clinical practice would be extremely beneficial, but at present direct measurement is not possible. In practice, there are few invasive or noninvasive monitoring techniques with which to evaluate or calculate this parameter. The end-systolic pressure-volume relationship (ESPVR; for details see below) is a fundamental description of systolic cardiac mechanics, with especial regard to the preload recruitable stroke work (PRSW) relationship. PRSW is another index of contractility, which is perhaps less influenced by other parameters. The stroke work is the area of the pressure-volume loop. For each pressure-volume loop derived by vena caval occlusion, the stroke work is plotted relative to its end-diastolic volume. The slope of the derived linear relationship is a measure of contractility independent of preload and afterload. The PRSW relationship reflects the overall performance of the left ventricle, combining the systolic and diastolic components. It follows that the degree of contractility can be assessed, but, unlike blood pressure, an ideal number or range to describe it can not be derived. Since ESPVR and PRSW are unique for each ventricle, these parameters more accurately measure changes in contractility. The greatest impediment to the clinical application of ESPVR and PRSW is the difficulty in measuring ventricular volume and inducing a preload reduction to derive the pressure-volume loops. More easily measurable indices of contractility have been actively sought.

Many clinicians use ejection fraction measurements to evaluate the cardiac contractility. However, the ejection fraction is influenced by preload and afterload alterations without any change in contractility. Depending on the loading conditions, hearts with a lower ejection fraction can produce a greater CO. Although roughly indicative of the cardiac reserve, the ejection fraction is an inconsistent marker for the overall cardiac function perioperatively.

1.3. Characteristics of microcirculation

An impairment of the microcirculation is the ultimate common denominator in all forms of circulatory disturbances, which become fatal without treatment. The microcirculatory function is the main determinant of adequate tissue oxygenation and organ function, and it has been recognized that maintenance of an adequate microvascular blood supply is critical for the survival and function of the reperfused tissues.

Microcirculation transports O_2 and nutrients to tissue cells, ensures an adequate immunological function and, in diseases, delivers therapeutic drugs to target cells. The microcirculation includes the smallest blood vessels of an organ where O_2 release to the tissues takes place, and consists of arterioles, capillaries and venules. The main cell types comprising the microcirculatory network are the smooth muscle cells and adjacent endothelial cells lining the inside of the microvessels, and the red blood cells, leukocytes and plasma components in the blood. The structure and function of the microcirculation are highly heterogeneous in different organ systems. In general, the driving pressure, arteriolar tone, hemorheology and capillary patency are the main determinants of capillary blood flow (Ince 2005).

The regulatory mechanisms controlling the microcirculatory perfusion are classified as myogenic, metabolic or neurohormonal. Myogenic control involves sensing strain and stress, while metabolic control is regulation based on O_2 , CO_2 , lactate and H^+ concentrations. This control system uses autocrine and paracrine interactions to regulate the microcirculatory blood flow to meet the O_2 requirements of tissue cells. The endothelial cells lining the inside of the microvessels play a central role in this control system by sensing flow, and metabolic and other regulating substances to regulate the arteriolar smooth-muscle-cell tone and capillary recruitment (Ince 2005).

Due to circulatory disturbances, such as hypovolemic or hemorrhagic shock (HS), when the oxygen delivery (QO_2) to a tissue is reduced, increases in O_2 extraction help to maintain the oxygen consumption (VO_2). However, below a critical delivery, the increases in O_2 extraction are inadequate to maintain VO_2 , which becomes limited by the O_2 supply. The

ability to optimally match the microvascular O_2 delivery with respect to the metabolic need helps to preserve the tissue VO_2 as QO_2 is reduced. If the capillary blood flow is not regulated in accordance with the O_2 needs, some capillaries will be underperfused while others are excessively perfused. When this occurs, the normal oxidative metabolism may continue as long as the overall QO_2 remains high. However, if the overall O_2 delivery were to decrease, cells in relatively poorly perfused regions could become O_2 supply-limited at a point where other cells in the tissue were still well supplied. When the systemic O_2 delivery is lowered by reducing CO, the baroreceptor and volume receptor reflexes augment the neurohumoral vasoconstriction in the tissues. This response helps to maintain the blood pressure and contributes to redistribution of the blood flow among the organ systems. Within the tissues, this vasoconstriction contributes to an increase in O_2 extraction, presumably by limiting blood flow to the capillaries with lesser metabolic demands and preventing a “microvascular steal” of the O_2 supply (Tsai 1993, Vollmar 1994).

1.4. Analysis of microhemodynamics

The recent development of new medical imaging techniques, together with data from clinical investigations, has helped to identify the microcirculation as playing a key role in pathological conditions. The most convincing data concerning the significance of this system derive from intravital microscopy (IVM) studies. This technology allows real-time imaging of the microcirculation and exact determination of the consequences of circulatory disorders. Disturbances of the microcirculatory perfusion are characterized by changes in the functional capillary density (FCD) and the red blood cell velocity (RBCV, $\mu m s^{-1}$). The FCD is defined as the length of red cell-perfused capillaries in relation to the observation area, which accurately describes the decrease in efficacy of tissue perfusion when the corresponding area is unchanged (Tsai 1995). The main causes of microcirculatory disturbances are as follows:

1. Changes in perfusion and vasoactivity

Microcirculatory dysfunctions seem to be mediated by endothelial cell damage and an imbalance of vasoconstrictor and vasodilator molecules, such as ET-1, nitric oxide (NO) and reactive oxygen species (ROS). These actions and pathophysiological events can result in decreases in FCD and RBCV. The hypoxia-induced extensive release of vasoconstrictor mediators can lead to significant vasoconstriction of the precapillary sphincters, *i.e.* a considerable proportion of the inflowing blood returns to the venules without passing through the capillaries. Precapillary vasoconstriction can also account for the relatively small decrease in arteriolar RBCV, which is determined primarily by the blood flow and the cross-section of

the circulatory area. In addition to precapillary vasoconstriction, other reperfusion-related factors, such as ROS production, can also contribute to the reduction of FCD and RBCV.

2. Cellular activity: leukocyte-endothelial interaction

Investigations utilizing IVM have demonstrated that the recruitment of inflammatory cells into the perivascular tissue involves a complex cascade mechanism. The adhesion process consists of several steps, beginning with the rolling of the polymorphonuclear leukocytes (PMNs) on the endothelial surface of the postcapillary venules until they have slowed down to such a degree that they stick to the endothelium. At this point, the PMNs are sequestered from the main vascular flow, and firm adherence to the endothelial cells may follow. Subsequently, the PMNs pass an intercellular junction between the endothelial cells and reach the abluminal side.

In general, reduced efficacy of the microcirculation results in a malfunction of the nutrient and waste product transport and leads to tissue damage. Simplifying terms, such as an impaired microcirculation, are generally used to describe this condition. However, this may rather misleadingly suggest that the microcirculatory responses are uniform in nature and similar in extent. In fact, macrocirculatory hypoperfusion can be associated with an increased flow heterogeneity leading to diverse distributions of O₂ between distinct anatomical structures of the intestinal wall (Cassuto 1979, Theuer 1993, Vallet 1994). Moreover, a second form of perfusion heterogeneity may be present when time-varying flow fluctuations evolve within the microvascular system of certain intramural structures (Madorin 1999).

Microcirculatory analysis is difficult in all tissue types when perfusion heterogeneity is present. Firstly, the conventional parameters of spatial heterogeneity (*e.g.* functional capillary density) and timewise heterogeneity (*i.e.* cycles min⁻¹) are insensitive to trace subtle microcirculatory alterations. Further, the comparison of velocities between continuous flow and pulsatile perfusion phases, between fast and slow-flow transition and between different flow patterns is impossible by this means. However, these microcirculatory alterations could be characterized by means of a probabilistic-based method of data analysis (Szabó 2004).

1.5. The vascular endothelium

Endothelial cells as the bricks of vascular lining are involved in many aspects of vascular biology, including vascular tone, hemostasis, immune and inflammatory responses, barrier function and angiogenesis. These functions range from relatively long-lived features to minute-by-minute responses to stimuli such as the synthesis and secretion of vasoactive mediators (Pearson 1991). The blood flow regulates the internal diameter of the arteries, both chronically through reorganization of the cellular and extracellular components of the

vascular wall, and acutely through relaxation/contraction of the smooth muscle cells. In both cases, the presence of the endothelium is required (Pohl 1986). Vasodilatation/vasoconstriction are regulated by many reflexes, neuronal and hormonal substances; they usually have systemic responses.

The endothelium is subjected to physical forces that are resisted by structural and dynamic features distributed throughout the cell. The structural elements associated with the luminal surface are responsible for the flow and the pressure sensor function of the endothelium (Davies 1992). The hemodynamic forces that act on the artery wall can be resolved into a pressure vector acting perpendicularly to the wall, and shear stress, the frictional force acting tangentially to the direction of flow. These forces can cause conformational changes in the luminal cell membrane to distort surface proteins, some of which are transmembrane integrins linked to the cytoskeletal elements on the intracellular side (Davies 1993a). Thus, the endothelium functions as a sensitive signal transduction interface between the flowing blood and the vessel wall. The stimuli of signal transduction are both the mechanical stress and the circulating vasoactive agonists (Davis 1993b, Hecker 1993).

In consideration of the local micro-environment, several vasoactive peptides and other products, such as the O_2 , CO_2 , K^+ and H^+ levels, play important roles in the circulation of organs and tissues. These effects contribute significantly to the development of pathophysiological processes. Many pathways, substances, hemodynamic stimuli and mechanical forces are triggers for the endothelium to synthesize vasoactive peptides and substances. Among them, two dominant factors, NO and ET-1, can significantly modify the local and systemic circulatory patterns and additionally influence the activity of other cell types in the circulation, such as cardiomyocytes or PMNs (Miller 1992, Kuchan 1993).

It should be emphasized that an endothelial dysfunction is not only associated with emergency circulatory disturbances: the pathological release of vasoactive peptides often leads to atherosclerosis and is common in patients with diabetes mellitus, hypertension or other chronic diseases.

1.6. Vasoregulatory role of endothelins

ET release is regulated by both rheological and chemical factors, such as pulsatile stretch, shear stress and pH (Malek 1992, MacArthur 1994, Wesson 1998). Hypoxia is considered one of the basic stimuli for ET synthesis (Rakugi 1990). Cytokines, adhesion molecules and vasoactive agents also stimulate ET production (Imai 1992, Bodin 1995). Under physiological conditions, ET is produced predominantly by the endothelium, but in

pathophysiological states other cells, such as PMNs, macrophages, smooth muscle cells, cardiomyocytes and mesangial cells, can also be the source of ET release (Ehrenreich 1990, Hahn 1990, Fukunaga 1991, Sessa 1991, Ito 1993).

ET isoforms are coded by at least three distinct genes; following transcription, ETs are formed by multiple cleavage via prepro-ET and then big-ET. The process may be influenced considerably by the activity of ET converting enzyme (ECE) isoforms present in endothelial, smooth muscle cells, cardiomyocytes and macrophages. Due to the functional and structural similarities with neutral endopeptidases, ECE-independent mechanisms may also contribute to ET production (Turner 1997). The process results in 21-residue peptide isoforms of ET-1, ET-2, and ET-3. The responsiveness to ET isopeptides is heterogeneous in a variety of vascular and nonvascular tissues.

Once the ETs are formed, their physiological and pathophysiological actions are mediated by at least two distinct receptor subtypes, ET-A and ET-B, both from the family of G-protein-coupled receptors. The ET-A receptor has a higher affinity for ET-1 and ET-2 than for ET-3, whereas the ET-B receptor displays equal affinities for all the isopeptides (Arai 1990, Sakurai 1990). The receptors mediate different circulatory effects, depending on their localization, but it is suggested that vasoconstriction is mediated predominantly via the ET-A subtype, while the activation of ET-B receptors elicits both vasodilator and vasoconstrictor responses (Clozel 1992, Sumner 1992, Shetty 1993).

In the vasculature, ET-A receptors are localized on smooth muscle cells, whereas ET-B₁ receptors are found on endothelial cells, and to a lesser extent, ET-B₂ in smooth muscle cells. ET-A receptors exhibit exclusive affinity for the ET-1 peptide, but ET-B receptors have no isoform preference. Stimulation of ET-A and ET-B₂ receptors leads to the activation of phospholipase C, with a subsequent accumulation of inositol triphosphate and intracellular Ca²⁺, resulting in vasoconstriction. In contrast, ET-B₁ receptors mediate the release of NO and prostacyclin and inhibit ECE expression in the endothelium. ET-B receptors are also involved in the clearance of circulating ET (Fukuroda 1994, Ozaki 1995).

The cardiac tissue has been shown to produce a number of substances that modulate myocardial contraction, including ET. The synthesis of ET occurs in both the vascular and cardiac chamber endothelium and by cardiac myocytes. The effects of ET on the heart are therefore thought to be paracrine and autocrine, at least in non-pathological states. Within isolated myocardial tissue, ET is a potent inotrope, with effective concentrations in the subnanomolar range. However, the *in vivo* relevance of these data remains unclear. The concentrations of ET that cause a positive inotropic effect in the heart have generally been

shown to cause coronary constriction. The resultant relative ischemia would potentially oppose any positive inotropy that ET would otherwise elicit (Battastini 1996). Moreover, it has been demonstrated that the plasma ET-1 levels correlate linearly with the amount of blood lost during HS (Chang 1993, Schlichting 1995). This suggests that the activation of vasoconstrictor ET receptors can further play a decisive role in acute microcirculatory disorders of the peripheral cardiovascular system.

Apart from other functions not listed here, ET is involved in bronchoconstriction (Uchida 1996) and contributes to inflammation processes either by stimulating cytokine production or by the direct induction of mast cell degranulation, neutrophil adhesion or platelet aggregation (Agui 1994, Yamamura 1994, Espinosa 1996, Boros 1998). The role of ET in these processes is supported by the fact that elevated plasma or tissue ET levels have been demonstrated in certain chronic cardiovascular diseases, such as congestive heart failure or atherosclerosis.

1.7. The ETR-p1/fl peptide

Specific blockade of ET receptors is a promising tool for elucidation of the role of the ETs in physiological regulation and in different pathological conditions. In a response to this demand, numerous ET receptor antagonists have been developed in the past decade. While some of these are nonselective, and inhibit both ET-A and ET-B receptors (*e.g.* bosentan; Gardiner 1994), other antagonists have specificity toward either the ET-A receptor (BQ-123, BQ-610, Ihara 1992, Ishikawa 1992) or the ET-B receptor subtype (IRL-1038, Karaki 1993). In consequence of the controversial effects mediated by ET-B receptors, a specific antagonist against the ET-B₁ receptor subtype has also been developed (RES-701-1; Tanaka 1994).

The ETR-P1/fl peptide is an antisense homology box-derived peptide with strong inhibitory potency against the ET-A receptor. The ETR-P1/fl peptide was developed by using the antisense homology boxes of the human ET-A receptor. The sense-antisense interaction means that the peptide synthesized from the inactive DNA strand is complementary to the peptide translated from the active DNA strand. Peptides therefore can recognize and bind to each other (Blalock 1984). Moreover, a sense-antisense interaction exists not only between individual peptides, but also within two parts of the one peptide chain. These amino acid sequences are termed antisense homology boxes (Baranyi 1995). In previous *in vitro* experiments, the ETR-P1/fl peptide induced relaxation in ET-1-precontracted vessel rings. The reference drug, the commercially available, highly specific ET-A receptor antagonist BQ-123, exerted the same effect in this setting, demonstrating the ET-A receptor-inhibitory property of the ETR-P1/fl peptide (Baranyi 1998).

1.8. Significance of fluid resuscitation in circulatory disturbances

In the treatment of acute circulatory failure, fast, efficient and self-tailored fluid replacement is a primary goal. The administration of intravenous fluid to avoid dehydration, maintain an effective circulating volume, and prevent inadequate tissue perfusion should be considered a core element of perioperative practice (Grocott 2005). The main goal of fluid therapy is to ensure an adequate O₂ supply for the organs.

Hypovolemia, as an absolute or relative blood volume deficit, is often encountered in surgical procedures, trauma and intensive care. Bleeding causes absolute volume deficits, and the vasodilation mediated by vasoactive substances is involved in producing relative volume deficits. It is well known that compensatory responses to hemorrhage lead to a disproportionate reduction in splanchnic blood flow during shock and this persists after resuscitation (Scannell 1992). The persistent splanchnic blood flow deficit is thought to contribute to the development of multiple organ failure (Faist 1983, Deitch 1990). The aim of primary resuscitation is reversal of the maldistribution of blood flow in the macro- and microcirculation. Despite restoration of the macrohemodynamics, several studies (Scalia 1990, Wang 1990, Scannell 1992) have shown that microcirculatory derangement still evolves and the flow deficit to splanchnic organs persists (Messmer 1989, Scalia 1992). These mechanisms have not been fully characterized to date.

The individual volume therapy during surgical procedures in normovolemic case often plays a crucial role in successful management. This essential role is also important throughout the perioperative phase (Vollmar 2004). Small volume resuscitation with hyperosmotic, colloid-crystalloid solutions effectively improves the cardiovascular function and has proved much more efficient than normotonic volume replacement (Velasco 1980, Kramer 1986, Armistead 1989). Hyperosmotic solutions cause a plasma volume expansion by withdrawing water from the extravascular space, reducing the extravascular pressure, increasing the circulating volume and creating favorable histological pressure conditions at the level of the capillaries (Frohlich 1966). As a result, they effectively improve the cardiovascular function and reduce the total peripheral resistance, thereby enhancing the capillary circulation, and improving the perfusion of the hypoperfused organs. In the long run, hyperosmotic solutions increase the amount of O₂ available in the body through increasing the blood pressure and CO and reducing resistance. According to the advanced trauma life support guideline (American College of Surgeons, Committee on Trauma, 1997), hypertonic solutions can restore the circulation effectively.

Dextran-based hyperosmotic solutions are known to be effective in restoring the macrohemodynamics (Dries 1996). If they are applied as hypertonic saline - dextran (HSD) solution, this effect can be enhanced, and at the same time swelling of the endothelial cells can be prevented (Mazzoni 1990). The dextran component also reduces leukocyte adhesibility, thereby preventing consequent capillary constriction (Nolte 1991, Menger 1993, Menger 1995). The most beneficial hemorheological properties of dextran are its inhibition of erythrocyte and thrombocyte aggregation and adhesion (Rutherford 1988), changing the surface polarization of erythrocytes and endothelial cells (Baldwin 1991), and decreasing the activity of Factor VIII (Bergentz 1978). According to recent studies, high-molecular-weight dextran (dextran-500) attaches to the endothelial surface more effectively than do low-molecular-weight dextrans (dextran-20, -40 and -70), which are commonly used in medicine (Gonzalez-Castillo 2002). The protective role of low molecular weight dextran may therefore become questionable.

The primary target organ of fluid replacement is the vascular endothelium. This surface is sensitive to the mechanical stimulus of blood flow and it can play a very significant role in resuscitation. This sensitive sensory and transmitter surface between the circulating blood and the wall of vessels (Hecker 1993) throughout the body is the site where several vasoactive mediators of endothelial origin are released and synthesized (Miller 1992, Kuchan 1993). Infused HSD solution presents a considerable mechanical stimulus for the endothelial cells, partly by increasing the shear stress affecting the surface, and also because of the hyperosmotic effect.

2. Main goals

The general aim of our studies was to analyze the effects of ET-A receptor antagonism on the central and peripheral circulatory patterns in physiological states and in conditions associated with endogenous ET-1 overproduction. In the first series of experiments, we set out to examine the consequences of rapid alterations in peripheral flow on the ventricular function with or without ET-A receptor antagonist treatment. To this end, we employed a hypertonic-hyperoncotic solution to induce rapid changes in the macro- and microhemodynamics.

Since a constant NO release will normally suppress ET production and action, we hypothesized that the nonspecific inhibition of nitric oxide synthase (NOS) unveils or enhances ET-1 effects. Hence, in the second series, we planned to characterize the consequences of artificially diminished NO production on the myocardial performance, and examined the ET receptor dependence of the process.

In a further series of experiments, the aim was to investigate the peripheral microcirculatory consequences of acute cardiovascular deterioration with ET-1 release in order to assess the efficacy of fluid therapies with or without ET-A receptor antagonist treatment.

- A.** Study I outlined the consequences of an HSD-40 infusion-induced peripheral flow stimulus on the ventricular function, together with detailed biochemical analyses of the myocardial tissue with or without ET-A receptor antagonist pretreatment.
- B.** Study II characterized the ET-A receptor dependence of artificially diminished NO production on the myocardial performance in a large animal model by using the nonselective L-arginine analog NOS inhibitor N- ω -nitro-L-arginine (NNA).
- C.** Study III assessed the microcirculatory efficacy of HSD with or without ET-A receptor antagonist treatment during acute circulatory deterioration and compromised peripheral perfusion.

3. Materials and Methods

The experiments were performed in adherence to the NIH guidelines for the use of experimental animals. The study was approved by the Ethical Committee for the Protection of Animals in Scientific Research at the University of Szeged.

3.1. Surgical preparation

The experiments were performed on a total of 84 inbred mongrel dogs (average weight 16.4 ± 2.8 kg). Anesthesia was induced with sodium pentobarbital ($30 \text{ mg kg}^{-1} \text{ iv}$) and sustained with $0.2 \text{ mg kg}^{-1} \text{ h}^{-1}$ supplementary doses. After intubation of the trachea, the animals were mechanically ventilated with room air (Harvard Apparatus, South Natick, MA, U.S.A.). The left femoral artery and vein were cannulated for the measurement of mean arterial pressure (MAP) and the administration of drugs and fluids, respectively. Blood gas parameters were regularly controlled throughout the experiments. The animals received $15 \text{ ml kg}^{-1} \text{ h}^{-1}$ Ringer's lactate infusion during the studies. In Study I, an identical dose of Ringer's lactate was given until the start of HSD treatment, while in Study III, the same dose of physiological saline infusion was given until HS induction. A Swan-Ganz thermodilution catheter (Corodyn TD-E-N, 5011-110-7Fr; Braun Melsungen AG, Melsungen, Germany) was positioned into the pulmonary artery via the right femoral vein to measure and calculate CO and cardiac index (CI).

In Studies I and II, an inflatable balloon-catheter (Foley catheter, 14Fr, Kendall Company Ltd., Basingstoke, U.K.) was introduced into the inferior caval vein via the left jugular vein. The filling volume was 10 ml. A catheter tip micromanometer (Millar Instruments Inc., Houston, TX, U.S.A.) was introduced into the left ventricle through the left internal carotid artery to monitor the left ventricular pressure (LVP). A left thoracotomy was performed at the sixth intercostal space and the pericardium was opened. A pair of ultrasonic dimension crystals (3 MHz, ID-4, Custom Transducers, Poway, CA, U.S.A.) were sutured onto the anterior and posterior walls of the left ventricle, opposite each other, using an atraumatic surgical technique for measurement of the left ventricular diameter (LVD). The thoracic cavity was revised and the chest wall was closed in four layers. The air was removed from the thorax; the animals were then breathing spontaneously. Their body temperature was maintained at 38°C with a homeothermic blanket. At the end of the experiments, a myocardial tissue biopsy sample was taken from the left ventricle and the animals were killed with an overdose of pentobarbital.

In Study III, involving animals with HS, blood was withdrawn through a catheter inserted into the right femoral artery. After a midline laparotomy, an ultrasonic flow probe

(Transonic Systems, Ithaca, NY, USA) was placed around the artery supplying the terminal ileum. Proximal to this enterotomy, the bowel was opened along the antimesenteric border, and placed on a pedestal, and the mucosal microcirculation was visualized with the Orthogonal Polarization Spectral (OPS) imaging technique. The exteriorized segment was continuously superfused with warm saline solution and covered with Saran wrap to avoid heat loss and evaporation.

3.2. Macrohemodynamic measurements

All hemodynamic signals (pressures, LVP and LVD) were registered with a computerized data-acquisition system (SPEL Advanced Haemosys 2.72, Experimetria Ltd., Budapest, Hungary). The MAP and central venous pressure (CVP) were monitored with Statham P23Db transducers. HR was calculated from the MAP curve. The CO was determined by thermodilution, using a Cardiostar CO-100 computer (Experimetria Ltd., Budapest, Hungary), normalized for body weight and expressed as CI ($\text{ml kg}^{-1} \text{ min}^{-1}$). The total peripheral vascular resistance (TPR) was calculated via the standard formula.

The ultrasonic dimension crystals were connected to a sonomicrometer (Triton Technology, Inc., San Diego, CA, U.S.A.). Via the LVP and LVD signals, the end-systolic elastance, as a parameter of the LV myocardial contractility, was estimated from the slope of the end-systolic pressure vs diameter relationship (Goldfarb 1982, Kaszaki 1996) with a computer program developed by our group (only in Studies I and II). The inferior caval vein was briefly occluded by a balloon catheter, and the pressure vs diameter loops were registered for 8 s. The end-systolic points of the loops (which can be fitted to a sigmoid curve) were recorded. The linear part of the curve was selected on the basis of the lowest variance, and a straight line was fitted to the selected points. The computer program calculated contractility as the slope of the end-systolic pressure vs diameter relationship, and the variance of fitting was determined. The calculation was based on a minimum of 8 cardiac cycles.

3.3. Microcirculatory measurements

The intravital OPS technique (Cytoscan A/R, Cytometrics, PA, USA) with a 10x objective was used for continuous visualization of the microcirculation of the intestinal villi. This technique utilizes reflected polarized light at the wavelength of the isobestic point of oxy- and deoxyhemoglobin (548 nm). Since polarization is preserved in reflection, only photons scattered from a 2-300 μm depth contribute to the image formation (Groner 1999). Images were recorded by an S-VHS video recorder (Panasonic AG-TL 700) and evaluated off-line by frame-to-frame analysis. FCD (length of perfused nutritive capillaries per observation area (cm^{-1}), and RBCV ($\mu\text{m sec}^{-1}$) were determined in 3 separate fields by means

of a computer-assisted image analysis system (IVM Pictron, Budapest, Hungary). During capillary flowmotion, RBCV was determined during high-flow and low-flow (or stop) conditions. All data were expressed as means of a minimum of 10 measurements at each time point.

3.4. Biochemical measurements

Plasma and cardiac tissue ET-1 measurements

Two-ml blood samples were drawn from the jugular vein into chilled polypropylene tubes containing EDTA (1 mg ml⁻¹) and aprotinin (Trasylol, Bayer, Leverkusen, Germany) (500 KIU/mL) before and after ETR-P1/fl peptide and NNA infusions, and at the end of the observation period. The blood samples were centrifuged at 1200g for 10 min at 4 °C. The plasma samples were then collected and stored at -70 °C until assay. For tissue samples (only in Study I), full-thickness heart biopsies were homogenized in phosphate buffer, and the homogenate was centrifuged at 4 °C for 30 min at 24 000g. The supernatants and plasma samples were analyzed for ET-1 with an ELISA kit (Biomedica, Vienna, Austria). According to the manufacturer, the cross-reactivity with ET-1 and ET-2 was 100%

NOS activity measurements

NO formation in cardiac tissues was measured via the conversion of [³H]L-citrulline from [³H]L-arginine according to the method of Szabó (1993). Briefly, heart biopsies kept on ice were homogenized in phosphate buffer (pH 7.4) containing 50 mM Tris-HCl, 0.1 mM EDTA, 0.5 mM dithiotreitol, 1 mM phenylmethylsulfonyl fluoride, 10 µg ml⁻¹ soybean trypsin inhibitor and 10 µg ml⁻¹ leupeptin. The homogenate was centrifuged at 4 °C for 20 min at 24 000g and the supernatant was loaded into centrifugal concentrator tubes (Amicon Centricon-100; 100 000 MW cut-off ultrafilter). The tubes were centrifuged at 1000g for 150 min and the concentrated supernatant was washed out from the ultrafilter with 250 µl homogenizing buffer. The samples were incubated with a cation-exchange resin (Dowex AG 50W-X8, Na⁺ form) for 5 min to deplete endogenous L-arginine. The resin was separated by centrifugation (1500g for 10 min) and the supernatant containing the enzyme was assayed for NOS activity.

For the Ca²⁺-dependent NOS (cNOS) activity, 50 µl enzyme extract and 100 µl reaction mixture (pH 7.4, containing 50 mM Tris-HCl buffer, 1 mM NADPH, 10 µM tetrahydrobiopterin, 1.5 mM CaCl₂, 100 U ml⁻¹ calmodulin and 0.5 µCi [³H]L-arginine (Amersham U.K., specific activity 63 Ci mmol⁻¹)) were incubated together for 60 min at 37 °C. The reaction was stopped by the addition of 1 ml ice-cold HEPES buffer (pH 5.5) containing 2 mM EGTA and 2 mM EDTA. Measurements were performed with the NOS

inhibitor NNA (3.2 mM) to determine the extent of [^3H]L-citrulline formation independent of the NOS activity. Ca^{2+} -independent NOS activity (iNOS) was measured without Calmodulin and with EGTA (8 mM). 1 ml reaction mixture was applied to Dowex cation-exchange resin (AG 50W-X8, Na^+ form) and eluted with 2 ml distilled water. The eluted [^3H]L-citrulline activity was measured with a scintillation counter (Tri-Carb Liquid Scintillation Analyzer 2100TR/2300TR, Packard Instrument Co, Meriden, CT, U.S.A.). Protein contents of samples were determined by the Lowry method.

Myocardial myeloperoxidase (MPO) activity measurement

The MPO activity, as a marker of tissue PMN leukocyte infiltration, was measured via cardiac muscle biopsies (Kuebler 1996). Briefly, the sample was homogenized with Tris-HCl buffer (0.1 M, pH 7.4) containing 0.1 mM phenylmethylsulfonyl fluoride to block tissue proteases, and then centrifuged at 4 °C for 20 min at 2000g. The MPO activities of the samples were measured at 450 nm (UV-1601 spectrophotometer, Shimadzu, Japan) and the data were referred to the protein content.

3.5. Experimental protocols

In Study I, surgery was followed by a recovery period for cardiovascular stabilization, and baseline variables were then determined during a 30-min control period. The animals were randomly allocated to one or other of three groups. Group 1 ($n = 10$) served as control and was treated with 0.9% saline (4 ml kg^{-1}), while Groups 2 ($n = 7$), and 3 ($n = 7$) were infused iv with 4 ml kg^{-1} HSD during 15 min. The solution was prepared from isotonic 10% dextran-40 (Baxter, Munich, Germany) and 7.2% NaCl solution. The animals in group 3 were additionally treated with the selective ET-A receptor antagonist ETR-p1/fl peptide (VLNLCALSVDYRAVASWRVI; Kurabo Ltd, Osaka, Japan (Baranyi 1995); 100 nmol kg^{-1} iv bolus in 1.5 ml kg^{-1} saline) 15 min before HSD treatment. The beginning of HSD infusion served as the zero point of the experiments, and the animals were observed for a further 120 min in all groups.

In Study II, the animals were randomly allocated to one or other of three groups. Surgery was followed by a recovery period for cardiovascular stabilization. Baseline variables were determined during a 15-min control period. Group 1 ($n=7$) was treated with 0.9% saline iv, while in Groups 2 and 3 ($n=7$ each), the animals received 4 mg kg^{-1} NNA (Sigma Chem. U.S.A.) in 2 ml kg^{-1} saline during a 15-min iv infusion. The animals in Group 3 were additionally pretreated (100 nmol kg^{-1} iv bolus in 1.5 ml kg^{-1} saline) with the selective ET-A receptor antagonist ETR-P1/fl peptide (Kurabo Ltd., Osaka, Japan) (Baranyi 1998) 30 min

before NNA treatment. The animals were observed for 135 min after the end of the treatment period; hemodynamic measurements were performed every 30 min.

In Study III, the animals were randomly assigned into 3 groups, which were subjected to HS (Groups 1-3). Surgery was followed by a 60-min stabilization period. Baseline variables were recorded for 30 min, and blood was then withdrawn from the femoral artery into a heparinized (25 IU ml^{-1}) reservoir until the MAP reached 40 mmHg. Blood was additionally withdrawn, or retransfused to maintain the set MAP value for 60 min. The animals were monitored for 180 min after HS. In Group 1 ($n=11$), the animals were resuscitated with 0.9% saline (150% of the lost blood volume) over 10 min, followed by a low-rate infusion of saline ($1 \text{ ml kg}^{-1} \text{ hr}^{-1}$). Group 2 ($n=10$) was treated with HSD (7.2% NaCl-10% dextran, 4 ml kg^{-1}) over 10 min, followed by a continuous infusion of saline ($1 \text{ ml kg}^{-1} \text{ hr}^{-1}$). The animals in Group 3 ($n=8$) were treated with the selective ET-A receptor antagonist ETR-p1/fl peptide (100 nmol kg^{-1} iv bolus in 1.5 ml kg^{-1} saline) 5 min before resuscitation and then HSD (4 ml kg^{-1} over 10 min) and saline infusion ($1 \text{ ml kg}^{-1} \text{ hr}^{-1}$) were given.

3.6. Statistical analysis

In Studies I and II, data analysis was performed with a statistical software package (SigmaStat for Windows, Jandel Scientific, Erkrath, Germany). Changes in variables within and between groups were analyzed by two-way ANOVA. Time-dependent differences from the baseline (time 0) for each group were assessed by the Holm-Sidak test, while in Study III, changes in variables within groups were analyzed by two-way ANOVA tests followed by the Bonferroni test. The Student-Newman-Keuls test was used for all pairwise comparisons of the mean responses between the different treatment groups. In the Figures, mean values and standard errors of means are given. P values < 0.05 were considered significant.

4. Results

4.1. Study I Cardiac and peripheral effects of HSD treatment

Initial effects of surgery

The concentration of the HSD solution and the optimal conditions for the volume expander protocol were determined in pilot studies (data not shown). In the control group, there were no significant hemodynamic changes as compared with the baseline values, and the ET-1 level did not change significantly during the 120-min observation period.

The HSD-induced peripheral circulatory reaction was characterized by MAP increases and a biphasic change in TPR: an initial decrease was followed by a return to the baseline during the early phase of the postinfusion period, and the TPR was significantly elevated at 120 min in the postinfusion period (Table I).

After the ETR-p1/fl peptide pretreatment, the HSD infusion caused a slight, nonsignificant rise in MAP for 45 min as compared with the baseline (15 min: 137 ± 6 mmHg vs baseline 123 ± 4 mmHg) or with the HSD-only group. This pretreatment did not influence the early, transient decrease in TPR, but significantly decreased the late TPR elevation observed in the HSD-only group (Table I).

Table I. Peripheral effects of saline, HSD, HSD + ET-A receptor antagonist pretreatment on MAP [mmHg] and TPR [$\text{mmHg ml}^{-1} \text{ min}^{-1} \text{ kg}^{-1}$] changes.

	-30 min	15 min	30 min	60 min	120 min
MAP					
Control	128 ± 4	125 ± 5	124 ± 5	125 ± 6	120 ± 5
HSD	129 ± 4	$143 \pm 3^{* \dagger}$	$139 \pm 3^{\dagger}$	136 ± 4	$134 \pm 3^{\dagger}$
ETR-p1/fl+HSD	123 ± 4	137 ± 6	134 ± 5	132 ± 6	126 ± 5
TPR					
Control	1.17 ± 0.08	1.13 ± 0.05	1.14 ± 0.06	1.16 ± 0.08	1.11 ± 0.08
HSD	1.24 ± 0.06	$0.94 \pm 0.05^{* \dagger}$	1.09 ± 0.06	1.21 ± 0.08	$1.37 \pm 0.06^{\dagger}$
ETR-p1/fl+HSD	1.24 ± 0.12	$0.85 \pm 0.09^{* \dagger}$	1.05 ± 0.11	1.16 ± 0.11	1.24 ± 0.13

Values are means \pm SEM; HSD: 7.2% NaCl–10% dextran-40; ETR-p1/fl: ET-A receptor antagonist; * $P < 0.05$ within group; $\dagger P < 0.05$ between groups vs control group;

The cardiac consequences of the HSD-induced volume loading included an increased LVD until 60 min of in the postinfusion period (Fig. 1), a significant increase in CI (Table II) together with a significant myocardial contractility elevation (lasting for 60 min; Fig. 2), and a

gradually elevated HR (Table II). The ETR-p1/fl peptide pretreatment resulted in a lower HR as compared with the HSD infusion, especially in the later postinfusion phase (149 ± 8 vs 175 ± 4). In this group, the CI had returned to the baseline level by the end of the observation period. The ET-A receptor antagonist pretreatment caused a noteworthy enhancement of the HSD-induced LVD increase ($7.5\pm 1.99\%$), but this preload index did not differ significantly from the result for the HSD-only group (Fig. 1). The ETR-p1/fl peptide pretreatment significantly inhibited the HSD-induced elevation in myocardial contractility (Fig. 2).

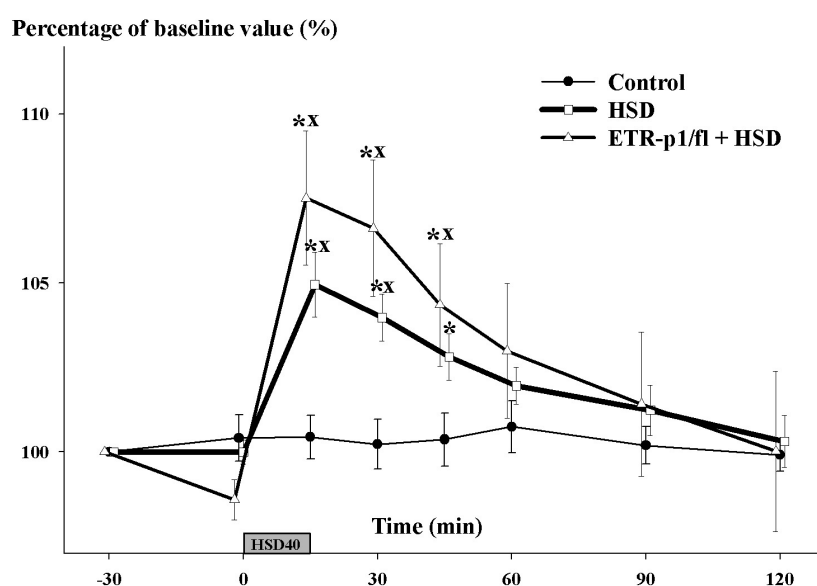


Figure 1. Changes in diastolic LVD in the saline-treated control group (black circles), the HSD-treated group (open squares) and the HSD+ETR-p1/fl-treated group (open triangles). Data are expressed as means \pm SEM. * $P<0.05$ within group; $^xP<0.05$

between groups vs saline-treated control group values. $^{\#}P<0.05$ between HSD-treated and ETR-p1/fl peptide+HSD-treated group values.

Table II. Cardiac effects of saline, HSD, HSD+ET-A receptor antagonist on CI [$\text{ml min}^{-1} \text{kg}^{-1}$] and HR [beat min^{-1}] changes.

	-30 min	15 min	30 min	60 min	120 min
CI					
Control	112 \pm 8	109 \pm 4	105 \pm 4	103 \pm 4	103 \pm 4
HSD	98 \pm 3	145 \pm 6* \dagger	122 \pm 6*	106 \pm 5*	91 \pm 5
ETR-p1/fl+HSD	105 \pm 8	167 \pm 12* \dagger \ddagger	133 \pm 9* \dagger	118 \pm 7	104 \pm 9
HR					
Control	155 \pm 6	153 \pm 6	156 \pm 6	155 \pm 6	160 \pm 5
HSD	158 \pm 5	163 \pm 4	162 \pm 5	171 \pm 4 \dagger	175 \pm 4* \dagger
ETR-p1/fl+HSD	157 \pm 8	152 \pm 5	149 \pm 6*	151 \pm 5 \ddagger	149 \pm 8* \ddagger

Values are means \pm SEM; HSD: 7.2% NaCl–10% dextran-40; ETR-p1/fl: ET-A receptor antagonist; * $P < 0.05$ within group; † $P < 0.05$ between groups vs control group; ‡ $P < 0.05$ between groups vs HSD-treated group;

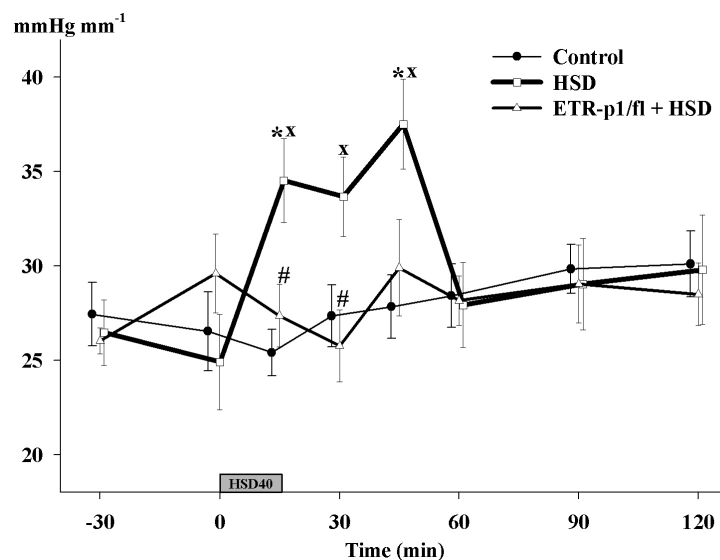
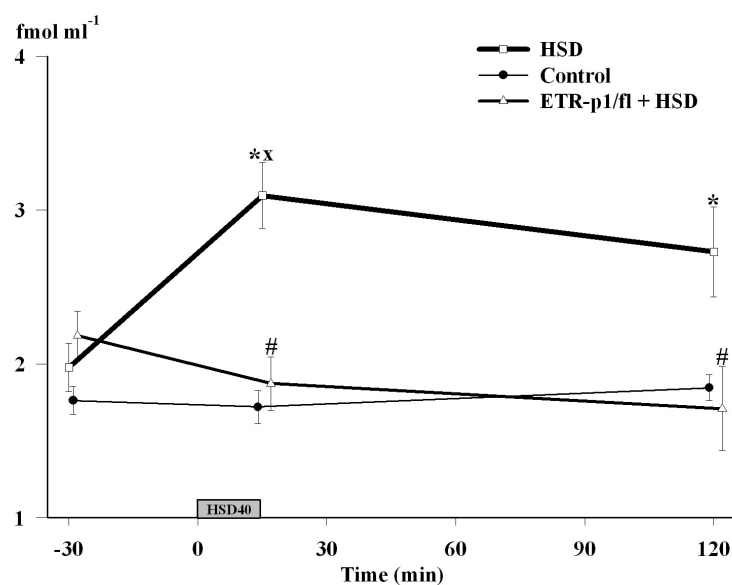


Figure 2. Changes in myocardial contractility in the saline-treated control group (black circles), the HSD-treated group (open squares) and the HSD+ETR-p1/fl-treated group (open triangles). Data are expressed as means \pm SEM. * $P < 0.05$ within group; ^x $P < 0.05$ between groups vs saline-treated control group values. # $P < 0.05$ between HSD-treated and ETR-p1/fl peptide+HSD-treated group values.

The plasma ET-1 concentration was significantly increased (approximately 1.5-fold) by the end of the infusion (HSD group: 3.095 ± 0.213 vs control group: 1.72 ± 0.107 fmol ml⁻¹), and remained significantly higher than in the control group up to the end of the 120-min



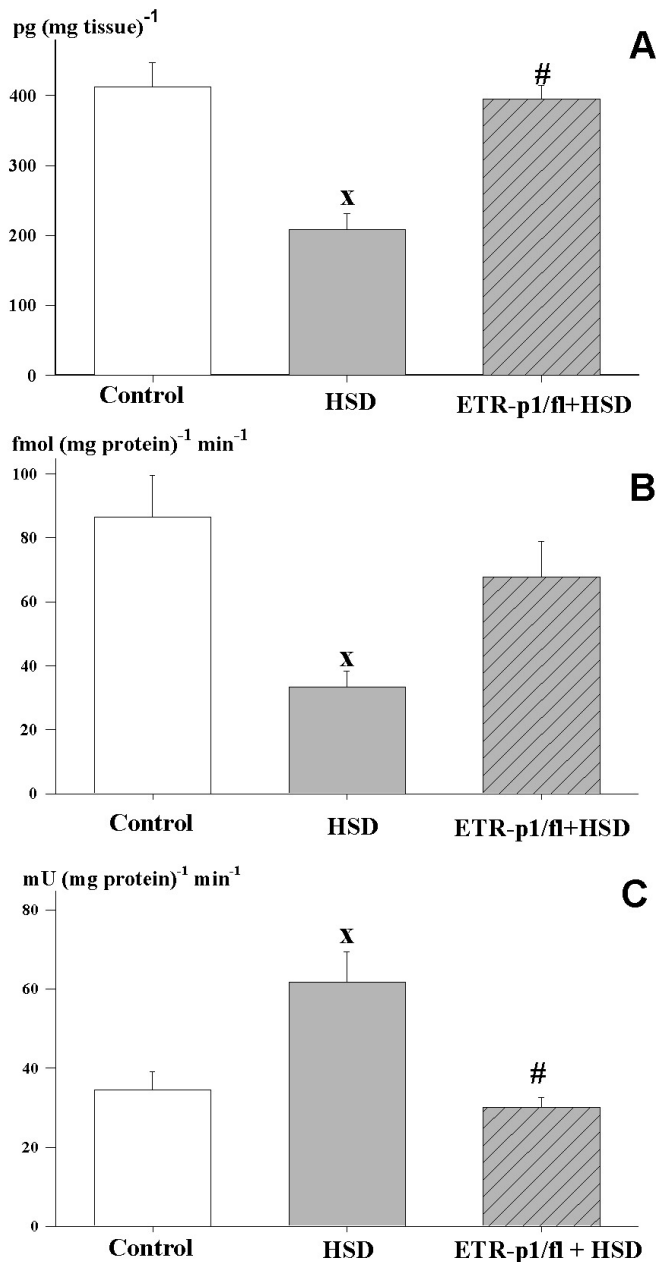
observation period. The ETR-p1/fl peptide pretreatment prevented the HSD-induced increase in plasma ET-1 level throughout the whole observation period (Fig. 3).

Figure 3. Changes in plasma ET-1 level in the saline-treated control group (black circles), the HSD-treated group (open squares) and the HSD+ETR-p1/fl-treated group (open triangles). Data are expressed as means \pm SEM.

* $P < 0.05$ within group; $^X P < 0.05$ between groups vs saline-treated control group values.
 $^{\#} P < 0.05$ between HSD-treated and ETR-p1/fl peptide+HSD-treated group values.

However, 120 min after the HSD infusion, the myocardial ET-1 content and cNOS activity were significantly lower as compared with those in the control group (Figs 4A and 4B). In these biopsies, the tissue MPO activity was significantly higher than in the control group (approximately 2-fold; Fig. 4C).

The ET-A antagonist pretreatment prevented the HSD-induced decrease in myocardial ET-1 content and the cNOS activity changes at 120 min in the postinfusion period, as the NOS values were not significantly different from those in the control group (Figs 4A and 4B).



The administration of the ET-A receptor antagonist decreased the tissue MPO activity (30.1 ± 2.6 vs 61.7 ± 7.6 mU (mg protein)⁻¹ min⁻¹). These differences were statistically significant as compared with the HSD group (Figs 4C).

Figure 4. Changes in ET-1 content (A), cNOS activity (B) and myocardial MPO activity (C) in myocardial tissue 120 min after treatment from saline-treated (empty box), HSD-treated (gray box with black lines), ETR-p1/fl peptide+HSD-treated (gray box with stripes) animals. Data are expressed as means \pm SEM. $^X P < 0.05$ between groups vs saline-treated control group values. $^{\#} P < 0.05$ between HSD-treated and ETR-p1/fl peptide+HSD-treated group values.

Study II Cardiac effects of decreased NO production

In the control group, there were no significant hemodynamic changes as compared with the baseline values during the 180-min observation period. The infusion of 4 mg kg⁻¹ NNA resulted in sustained increases in MAP. The ETR-P1/fl peptide pretreatment mitigated the NNA-induced MAP elevations, but the differences between the values for the NNA and ETR-P1/fl peptide+NNA groups were statistically not significant (Fig. 5).

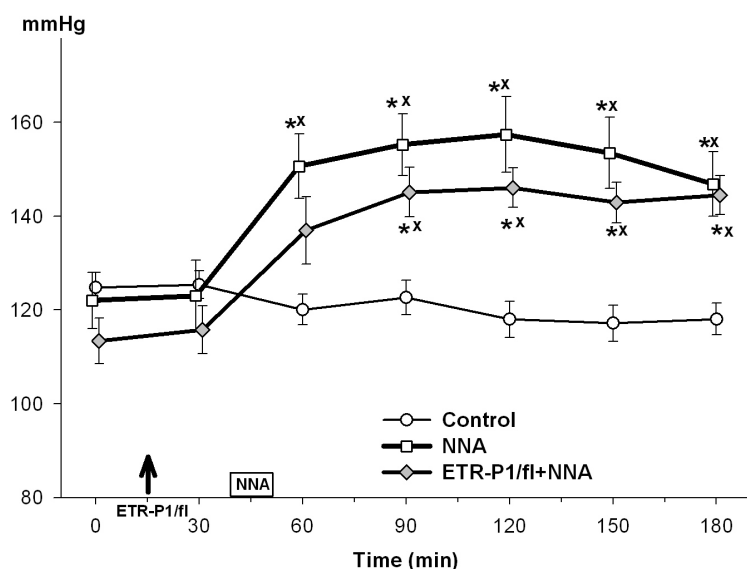


Figure 5. Changes in MAP in the control group (black circles), the NNA-treated group (open squares) and the ETR-P1/fl + NNA-treated group (gray diamonds). **P* < 0.05 within group; ^x*P* < 0.05 between groups vs saline-treated control group values.

Nonspecific NOS inhibition caused an ~ 25% decrease in CI (Fig. 6), while the difference between the LV diastolic and systolic diameters (as a percentage of the baseline) was also reduced significantly (Fig. 7). The cardiac effects of ET-A receptor antagonist pretreatment included an immediate, significant increase in CI at 30 min of the experiment (Fig. 6). Moreover, ETR-P1/fl peptide pretreatment significantly inhibited the NNA-induced decrease in CI and the LV diastolic-systolic diameter difference (Figs 6 and 7).

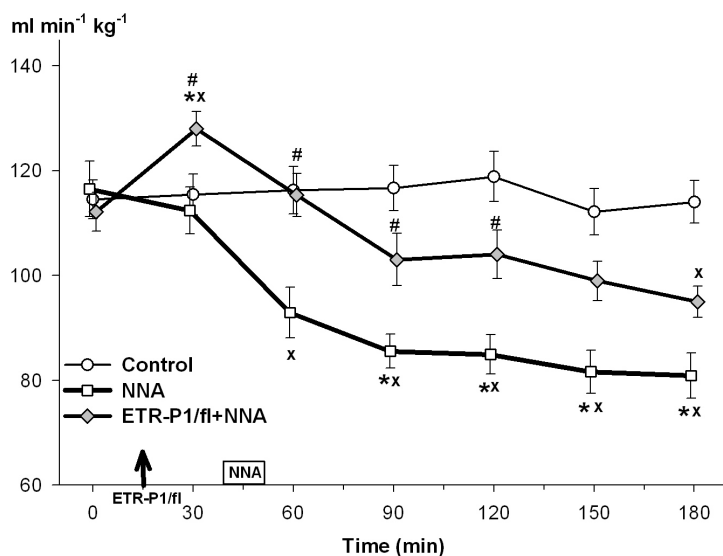


Figure 6. Changes in CI in the control group (black circles), the NNA-treated group (open squares) and the ETR-P1/fl + NNA-treated group (gray diamonds). **P* < 0.05 within group; ^x*P* < 0.05 between groups vs saline-treated control group values; #*P* < 0.05 between groups vs NNA-treated group values.

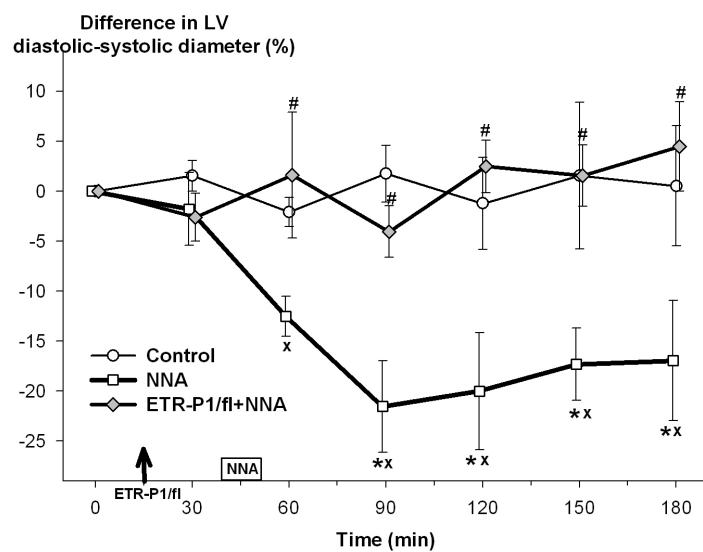


Figure 7. Changes in the LV diastolic-systolic diameter difference in the control group (black circles), the NNA-treated group (open squares) and the ETR-P1/fl + NNA-treated group (gray diamonds). * $P < 0.05$ within group; $^xP < 0.05$ between groups vs saline-treated control group values; # $P < 0.05$ between groups vs NNA-treated group values.

Nonspecific NOS inhibition caused a significant increase in myocardial contractility up to the end of the observation period. However, ETR-P1/fl peptide pretreatment significantly inhibited the NNA-induced decrease elevation in myocardial contractility (Fig. 8).

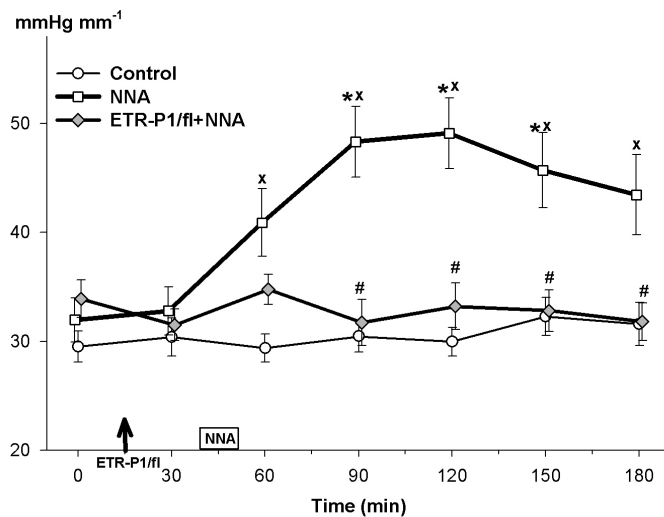


Figure 8. Changes in myocardial contractility in the control group (black circles), the NNA-treated group (open squares) and the ETR-P1/fl + NNA-treated group (gray diamonds). * $P < 0.05$ within group; $^xP < 0.05$ between groups vs saline-treated control group values; # $P < 0.05$ between groups vs NNA-treated group values.

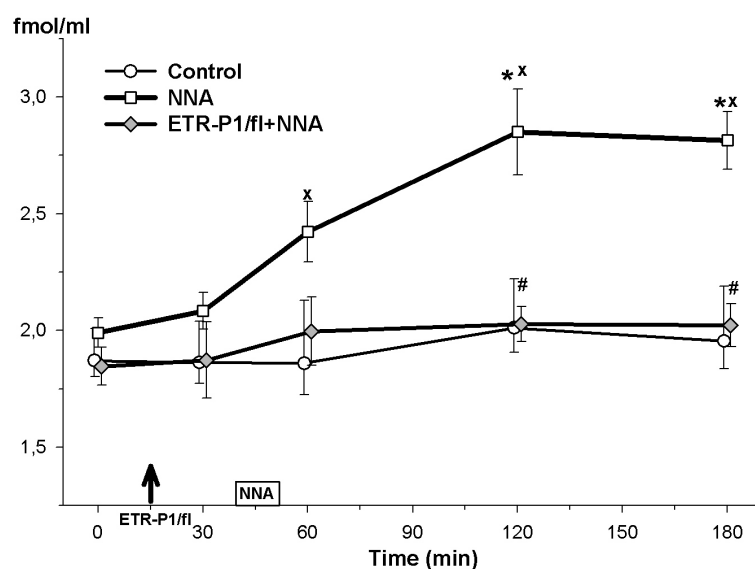


Figure 9. Changes in plasma ET-1 level in the control group (black circles), the NNA-treated group (open squares) and the ETR-P1/fl+NNA-treated group (gray diamonds). * $P < 0.05$ within group; $^xP < 0.05$ between groups vs saline-treated control group values; $^{\#}P < 0.05$ between groups vs NNA-treated group values.

The plasma ET-1 concentration gradually rose to approximately 1.5-fold following NNA infusion and remained significantly higher than in the control group up to 120 min in the observation period. The ETR-P1/fl peptide pretreatment prevented the NNA-induced increase in plasma ET-1 level throughout the observation period (Fig. 9).

Study III Effects of HSD and ET-A receptor antagonist treatment in hemorrhagic shock

Macrocirculatory changes

In the sham-operated group, the macro- and microhemodynamic parameters did not change significantly during the 330-min observation period (data not shown). Macrohemodynamic data on the treated groups are presented in Fig. 10A-C. During HS blood was additionally withdrawn or retransfused to maintain the set MAP value between 40-45 mmHg for 60 min (Fig. 10A). The ~ 50% reduction in the calculated blood volume was accompanied by an ~ 70% decrease in CI (Fig. 10B). Resuscitation was followed by a partial recovery in MAP, irrespective of the therapy applied. Resuscitation with saline resulted in a short-term restoration of CI at the onset of resuscitation, but this was followed by a gradual decline. A similar macrohemodynamic deterioration was observed after HSD treatment. ET-A antagonisms, however, resulted in a lesser degree of recovery in CI as compared with saline or HSD treatment at the onset of reperfusion (Fig. 10B). The ET-A antagonist treatment did not influence the HR (data not shown).

The intestinal perfusion was reduced by ~ 70% during HS. Although the blood flow exceeded the baseline after the start of resuscitation with saline, a gradual deterioration was then observed, parallel to the CI changes (Fig. 10C) and no difference was detected between the experimental groups after 15 min.

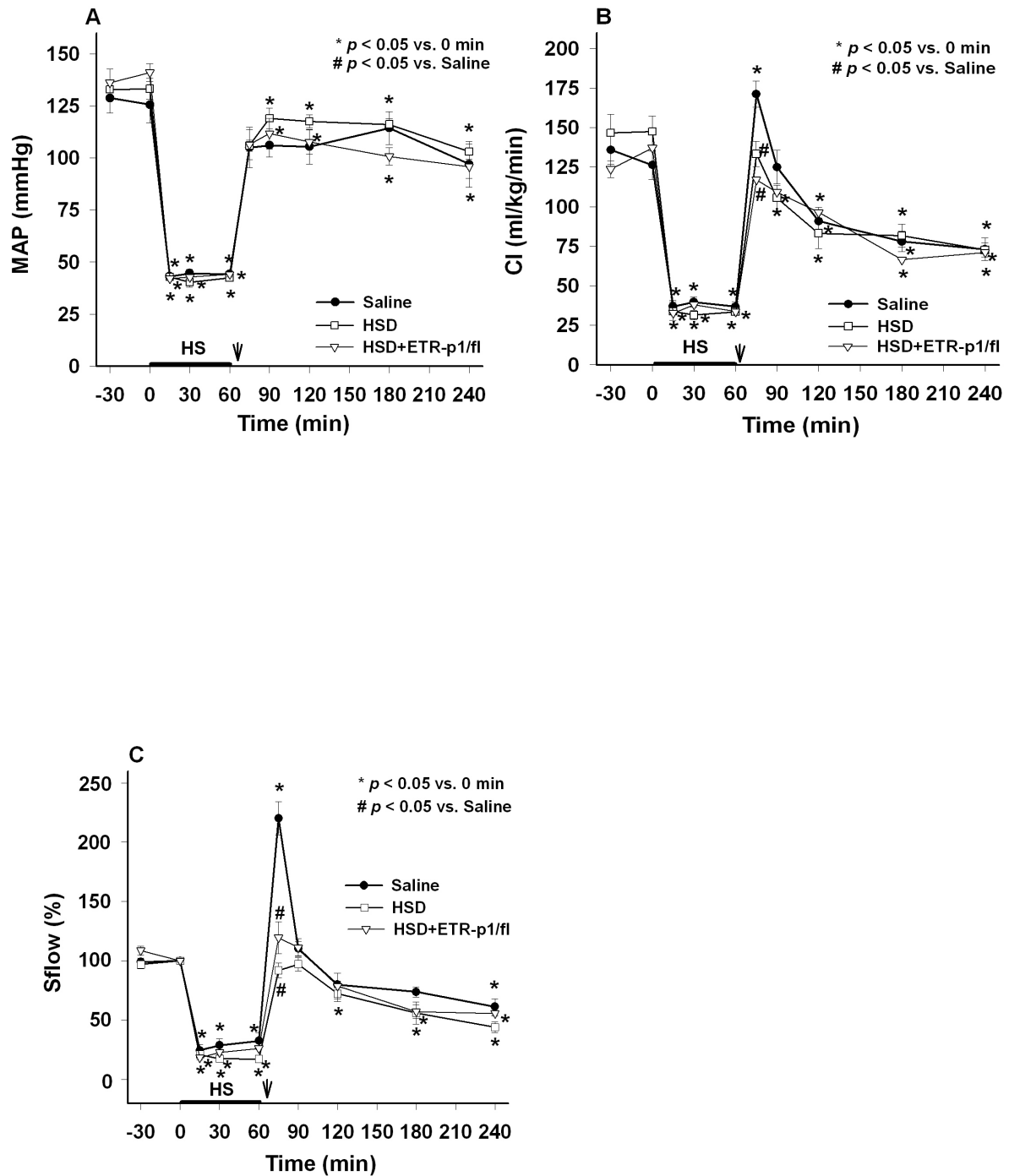


Figure 10. Macrohemodynamic changes during 60-min HS and 180-min resuscitation. MAP (A), CI (B) and segmental ileal blood flow (Sflow, C) in saline (black circles)-, HSD (open squares)- and HSD + ET-A receptor antagonist (open triangles)-treated groups.

Microcirculatory changes

Microcirculatory flow was continuous at the villus tips under the control conditions, while cyclic fluctuation appeared during HS. This time-dependent flowmotion was not confined to the capillaries: it could be also observed in subepithelial venules and central arterioles. Additionally, alternating (on-off) flow evolved within adjoining villi, *i.e.* spatially and temporally synchronized flow periods were observed.

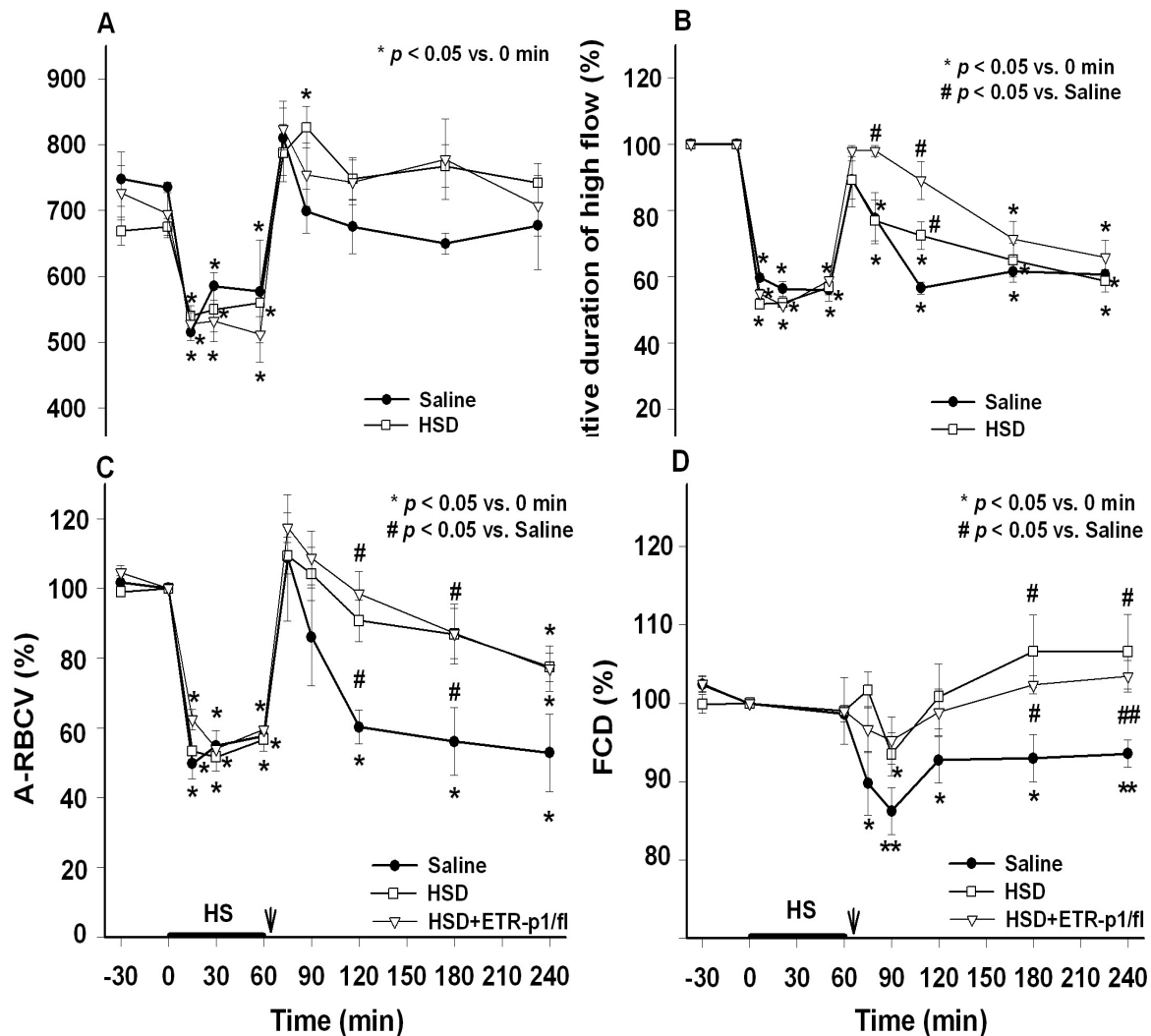


Figure 11. Microhemodynamic changes during 60-min HS and 180-min resuscitation. Changes in RBCV during high flow in the capillaries (A), relative duration of high-flow periods (B), A-RBCV (C), and FCD (D) in saline-(black circles), HSD-(open squares) and HSD + ET-A receptor antagonist-treated (open triangles) groups.

During HS, the RBCV during the high-flow phases was significantly lower than at the baseline (Fig. 11A), and returned to the control level in all groups at the onset of resuscitation. However, the RBCV was moderately higher in the HSD and HSD + ETR-p1/fl-treated groups

during the high-flow periods. A-RBCV (which allows simultaneous consideration of RBCV and the flow pattern changes) was restored at the onset of resuscitation in response to HSD and HSD + ETR p1/fl treatments (Fig. 11C).

Capillary stasis in hemoglobin-containing structures was not observed during HS. Resuscitation was associated with a decrease in FCD in each group, and a return to the control level was observed only in the HSD and HSD+ETR-p1/fl-treated groups (Fig. 11D).

During HS, periods of high RBCV ($\sim 500\text{-}600 \mu\text{m s}^{-1}$, Fig. 11A) were followed by periods of low RBCV ($\sim 100\text{-}150 \mu\text{m s}^{-1}$). The average duration of high and low-flow periods was 9.9 ± 0.4 and 7.4 ± 0.5 s, respectively. For a 60-s interval, this equals $3.5 \text{ cycles min}^{-1}$, or corresponds to an $\sim 43\%$ decrease in relative duration of high-flow periods as compared with the continuous baseline flow (100%). At the onset of resuscitation, continuous flow periods were transiently seen in 33%, 40% and 50% of the experiments after saline, HSD and HSD + ETR p1/fl treatment, respectively. During the later stages of resuscitation, the relative duration of high RBCV periods was decreased, indicating the predominance of oscillatory flow in the villi (Fig. 11B).

The ET-A receptor antagonism significantly increased the relative duration of the high-RBCV periods at the onset of resuscitation by prolonging either the continuous flow or the duration of high-flow periods during oscillation. In the event of prolonged high-flow periods, the use of cycles min^{-1} to express the periodicity would be particularly misleading since it would underestimate or mask these favorable alterations (Table III).

Table III. Comparison of data obtained from calculation of the relative duration of high-flow periods with those for the cycles. Data at 60 min of resuscitation ($t = 120 \text{ min}$) are shown.

Groups	Relative duration of high-flow	Cycles min^{-1}
Saline	0.56 ± 0.02 ($n = 11$)	4.11 ± 2.3 ($n = 11$)
HSD	0.72 ± 0.04 ($n = 10$)**	4.38 ± 2.0 ($n = 10$)
HSD + ETR-p1/fl	0.89 ± 0.06 ($n = 8$)*#	3.08 ± 1.6 ($n = 5$)

Values are means + SEM; n = numbers of animals, HSD, 7.2% NaCl-10% Dextran; ETR-p1/fl, ET-A receptor antagonist. * $P < 0.05$, ** $P < 0.01$ vs saline; # $P < 0.05$ vs HSD.

The plasma ET-1 level was elevated significantly by the end of the shock period in each group (from $3.93 \text{ pg ml}^{-1} \pm 0.52$ to $6.77 \pm 0.5 \text{ pg ml}^{-1}$; $P = 0.0016$). At the onset of resuscitation, the high level of ET-1 persisted in both HSD-treated groups, but, a decrease occurred in response to resuscitation with saline (to $2.87 \pm 0.71 \text{ pg ml}^{-1}$; $P = 0.353$ vs. baseline;

$P<0.05$ vs HSD groups). These changes were followed by a gradual increase until the end of the examination period in each group, reaching maximal values of 8.95 ± 2.86 pg ml⁻¹ in the saline-, 12.84 ± 1.68 pg ml⁻¹ in the HSD- and 12.12 ± 1.94 pg ml⁻¹ in the HSD+ETR p1/fl-treated groups, respectively (Fig. 12).

HS followed by 180 min of resuscitation was accompanied by a 54.2%, 116.4% and 52.4% increase in MPO activity in the intestine in animals resuscitated with saline, HSD, and HSD combined with the ET-A receptor antagonist, respectively (from 2.25 ± 0.25 to 3.47 ± 0.43 , 4.87 ± 0.82 ; $P<0.05$ vs baseline and 3.43 ± 0.72 U mg⁻¹ protein, respectively).

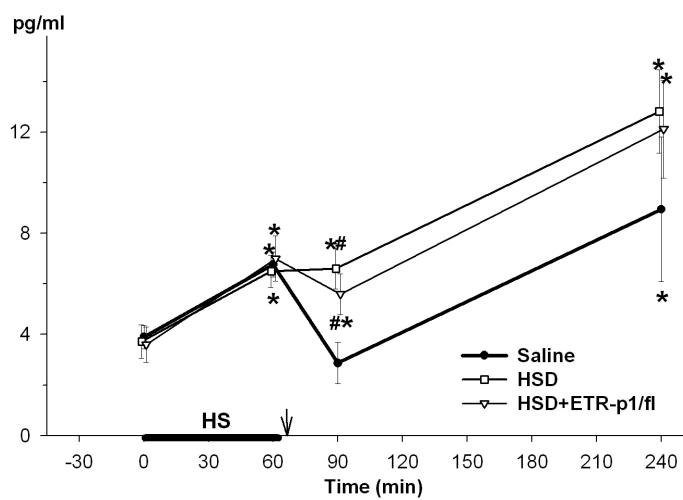


Figure 12. Changes in plasma ET-1 level in saline- (black circles), HSD- (open squares) and HSD + ET-A receptor antagonist- treated (open triangles) groups.

5. Discussion

In our research protocol we used the ESPDR as a preload-independent index of cardiac contractility (Goldfarb 1990), in order to study the circulatory effects of volume therapies. The results of our first experimental series (Study I) revealed the early and late consequences of HSD infusion on cardiac contractility alterations, and confirmed the potential connection between cardiac NO synthesis and ET-1 release. In general, hypertonic–hyperoncotic solutions bring about rapid changes in the macro- and microhemodynamics in various circulatory beds. This could be related to a number of mechanisms, including the redistribution of fluid from the interstitium to the intravascular space; a direct relaxing action on the vascular smooth muscle; a blood fluidity improvement by hemodilution and a stretch-induced ventricular dilatation caused by a pressure or volume overload (Janicki 2006). In our experiments, the molecular weight of the dextran component of the hyperosmotic–hyperoncotic solution was 40 kD. *In vivo*, solutions of 40 kD dextran are advantageous when an improvement in blood flow is specifically required, while a higher molecular weight dextran (*e.g.* 70 kD) is preferable when a longer circulation time and a plasma volume expansion are the primary goals. The rationale of our approach was to achieve a rapid increase in flow velocity. Indeed, the HSD infusion resulted in prompt increases in MAP and CO and a decrease in peripheral resistance; the HR concomitantly increased, and a significant rise in myocardial contractility was noted in the early phase of the postinfusion period.

The increased LV preload might contribute to the positive inotropy, but the mechanism of the HSD-induced myocardial contractility elevation is rather complex, and this change can not be a simple consequence of an increased intravascular volume. This hemodynamic pattern could increase the coronary blood flow too (*Gregg effect*), which itself could lead to positive inotropy (Gregg 1963, Feigl 1983), and reflex autonomic changes could additionally be involved in this process (Murray 2004).

The postinfusion period was characterized by significant rises in the plasma NO (see Annex §1) and ET-1 concentrations. Given the strong positive inotropic and chronotropic effects of ET-1 (Beyer 1996), it was important to determine how much of the HSD-induced contractility change was due to ET-1. In the later phase of the postinfusion period, the TPR increased significantly. In parallel with this, the HR gradually increased, while the CI decreased and the myocardial contractility returned to a near-baseline level. The increased frequency was probably due to the positive chronotropic effects of the released ET-1. As NO plays a vital role in controlling myocardial contractility, its lack could modify the regulation

to a great extent. Since both ET-1 and NO take part in the regulation, their ratio and the bioavailability of these vasoactive mediators are of crucial importance at any given moment.

ET-1 release and ET-1 effects on cardiac contractility

It has been shown that an acute volume expansion caused by a rapid infusion of hypertonic colloid solution results in an increase in plasma ET-1 (Boldt 1994). ET-1 release or synthesis is triggered by various mechanical stimuli, such as the increased osmolarity caused by cell shrinkage (Warner 1999), fluid shear stress on the endothelium (Fissthaler 2000, Kuchan 1993) and physical stretching of smooth muscle vascular cells or cardiomyocytes (van Wamel 2001).

Several aspects of the employed model highlight that the HSD-induced circulatory responses are characterized by predominantly ET-related immediate hemodynamic changes, demonstrating that this peptide is an important determinant of the increase in cardiac contractility, but ET-1-associated late cellular events can lead to a depressed cardiac function. Exogenous ET-1 infusion may increase the *in vivo* cardiac contractility significantly, an effect that can be prevented by ET-A receptor antagonist pretreatment (Konrad 2005). The results revealed that the plasma level of ET-1 increased significantly in this setup too, and the peptide induced positive inotropy through the activation of ET-A receptors. ET-1 undergoes mainly abluminal release, and its half-life in the circulation is very short as a consequence of effective eliminating mechanisms. The plasma ET-1 level subsequently remained elevated until the end of the experiment, which may suggest that, after induction by HSD, it was continuously replaced from the endothelium or myocardial cells. This possibility is supported by a decreased level of myocardial ET-1 content at the end of the postinfusion period. It should be noted that the positive inotropic ET-1 effect is usually observed only *in vitro*, because this phenomenon is antagonized by the ET-induced myocardial vasoconstriction and subsequent ischemic cardiodepression (Beyer 1996).

Significance of NO on cardiac contractility

The role of myocardial NO production in regulating the cardiac function is complex and controversial. Previous studies have indicated that excessive NO delivery from inflammatory cells (or cytokine-stimulated cardiomyocytes themselves) may result in profound cellular disturbances leading to attenuated cardiac contractility (Massion 2003). However, others have reported that the stimulation of myocardial NO production can offset the increase in contraction in response to a rise in intracellular Ca^{2+} . Cardiac NO production is also activated by stretching and under these conditions NO has been shown to facilitate the

Frank-Starling response and to contribute to the increase in intracellular Ca^{2+} transients that mediates the slow increase in contraction in response to a stretch (Casadei 2003).

However, a considerably decreased NOS activity was observed in the later postinfusion period, to the accompaniment of a TPR elevation and a CI decrease. This marked decrease in NOS activity may be an indirect consequence of the elevation in ET-1 level. It has been proved in a number of diseases involving circulatory failure (myocardial infarction, cardiogenic shock, atherosclerosis and congestive heart failure) and also in surgical interventions that an increased ET-1 level is associated with decreased NO production (Szabó 1993). One possible explanation of this phenomenon is that the HSD-induced ET-1 release may be attributed to an increase in superoxide radical production, simultaneously with significant NO production, and this leads to the formation of peroxynitrite, a known inhibitor of NOS activity (Sheehy 1998, Ovadia 2002). Furthermore, ET-1 *per se* could inhibit endogenous NO synthesis through enhanced asymmetric dimethylarginine synthesis and ET-A receptor activation (Ohnishi 2002). On the other hand, peroxynitrite-mediated myocardial protein nitration has been associated with a depressed cardiac pump function. Borbely *et al.* proposed that alpha-actinin is a target for peroxynitrite in the human myocardium; and its nitration can induce a contractile dysfunction (Borbely 2005). Additionally, an *in vivo* interaction might occur between the increased nitrite level and myocardial MPO, affording reactive nitrosyl derivatives (Dvorak 1986).

ET-A receptor antagonism

The ETR-p1/fl peptide used in our study has a special feature: it is an intramolecular complementary peptide of the ET-A receptors; as such, it can specifically recognize and bind the circulating ET-1 molecules, and it is thereby able to decrease the plasma level of released ET-1 (Baranyi 1995, 1998). ET-A receptor antagonism by the ETR-P1/fl peptide proved effective in reducing the signs of vasoconstriction and it protected the myocardium from excess energy use. As a result of ET-A receptor antagonist pretreatment, the CI did not decline below the control level, and TPR was not increased at the end of the postinfusion period. Moreover, the plasma level of ET-1 was significantly lower and in this case the positive inotropic and chronotropic effects were missing. This group was characterized by a high LVD: the filling volume increased as a result of inhibition of the ET-A receptor-induced venoconstriction. Hence, the volume per cardiac cycle increased, which maintained sufficient perfusion. Pretreatment with the ETR-p1/fl peptide has a protective role in maintaining the myocardial NOS activity and preserving the cardiac ET-1 content too, and the PMN accumulation in the cardiac tissue was also reduced. In summary, the data reported here

demonstrate that mechanical stimuli involving an HSD-induced volume expansion cause significant peripheral ET-1 release. This response may lead to an ET-1 - NO imbalance, an unfavorable side-effect of HSD fluid therapy, where ET-A receptor-associated effects predominate.

Our next study (Study II) was designed to explore the connection between basal NO synthesis and myocardial function in the unstressed dog, and we have shown that aspecific NOS inhibition leads to an increased myocardial contractility in this setting. The results revealed that the lack of NO is accompanied by significant ET-1 release. These experimental data therefore suggested a suppressive, regulatory role for endogenous NO: it restrains or counteracts these mechanisms, which would otherwise increase the cardiac contractility.

Hemodynamic effects of NOS inhibition

Our study has demonstrated the efficacy of NNA-induced NOS inhibition together with prolonged increases in MAP and total peripheral vascular resistance, and decreased CI. NOS inhibitor treatment caused a decrease in the LV diastolic-systolic diameter difference, which points to an attenuation of the Frank-Starling response and might explain the decrease in CI (Prendergast 1997). Consistent with earlier results (Kaszaki 1996), NNA treatment caused a significant increase in heart contractility. Indeed, a detailed analysis of our experimental data suggested that the mechanism of the NNA-induced myocardial contractility elevation is a complex process which involves several variables. Experiments with NO donors have often shown the opposing effects of NO on the myocardial contraction and HR. It has been revealed that the reaction is biphasic and dose-dependent, *i.e.* low concentrations of NO donors (0.1-10 mM) increase the contractility and HR, whereas higher concentrations (> 100 mM) elicit negative inotropic and chronotropic effects (Casadei 2003, Massion 2003, Gonzalez 2008). Taken together, an important consequence of NOS inhibition could be an imbalance in the positive-negative inotropy (vasoconstrictor-vasodilator) relationship, which is shifted in the direction of positive inotropy.

ET-1 release and ET-1 effects on cardiac contractility

We have shown that a diminished NO synthesis leads to a preponderant ET-1 effect. Since NO may normally moderate ET-1 production and action (Boulanger 1990, Kourembanas 1993), the inhibition of NO synthesis can result in increased plasma levels of ET-1 (Richard 1995, Filep 1997). It has been demonstrated that, after acute NOS blockade, the predominant pressor mechanism is associated with a marked increase in ET-A/ET-B receptor activation, rather than with increases in alpha-1, angiotensin 1 or vasopressin V1/V2 receptor activation (Banting 1996).

Several aspects of the model highlight that the NNA-induced circulatory responses are characterized by predominantly ET-related immediate hemodynamic changes, demonstrating that this peptide is an important determinant of the increase in cardiac contractility. This observation supports the *in vitro* finding that NOS inhibition enhances the inotropic response to ET-1 (Kinnunen 2000). Exogenous ET-1 infusion may increase the *in vivo* cardiac contractility significantly, an effect that can be prevented by ET-A receptor antagonist pretreatment (Konrad 2005). In our study, the plasma ET-1 level gradually increased up to the end of the experiments, which may suggest that, after induction by NNA treatment, it was continuously replaced from the cellular sources. The results also revealed that the ET-1 peptide induced positive inotropy through the activation of ET-A receptors. Recent evidence strongly suggests that the target area of NO and/or ET-1 is the same cellular microdomain for the modulation of cardiomyocyte contractility, via regulation of the L-type Ca^{2+} channels, but in the opposite sense (Casadei 2003, Robu 2003).

ET-A receptor antagonism

ET-A receptor antagonism by the ETR-P1/fl peptide proved effective in reducing the signs of vasoconstriction. As a result, CI displayed an immediate significant increase and did not decline below the control level following NNA treatment, while the NOS inhibition-induced elevation in total peripheral vascular resistance was lowered. This observation is in agreement with the data of Maeda *et al.* (2004), who demonstrated that an exercise-induced increase in ET-1 significantly lowered the plasma NO concentration in the kidney, whereas pretreatment with an ET-A receptor antagonist resulted in significantly higher NO production (Maeda 2004). This elevation in NO production, presumably through activated ET-B receptor-induced NO release (Verhaar 1998), plays a role in normalizing the LV diastolic-systolic diameter difference. Additionally, the plasma level of ET-1 was significantly lower and in this case the positive inotropic effect was missing. Hence, the volume per cardiac cycle increased, which maintained sufficient perfusion.

It has been shown that ETR-p1/fl peptide infusion in the same dose induces significant increases in CI, LV systolic-diastolic difference and significant decreases in TPR and plasma ET level, while it does not influence MAP, HR and cardiac contractility (Kaszaki 1997).

It should be noted that direct and indirect (or peripheral and central) effects of NOS and ET antagonism are difficult to distinguish *in vivo*. Taken together, the increase in LV contractility could be due to several factors, including increases in preload and coronary blood flow or the effects of reflex autonomic changes (*e.g.* baroreceptor responses). However, the results underline the significance of diminished NO production in ET-1 release, and these

processes could contribute indirectly to the alterations in cardiac contractility through ET-A receptor activation.

In our further research protocol (Study III), the intestinal macro- and microcirculatory consequences of a 50%-blood volume reduction and the effects of low-volume resuscitation were investigated. The severity of hemorrhage was marked by ~70% decreases in CO and ileal blood flow, together with a significant overproduction of ET-1 in the plasma. Resuscitation caused a partial and transient restoration in macrohemodynamics, which was followed by a gradual deterioration irrespective of the applied therapy. Nevertheless, hypertonic solutions induced a significant microcirculatory improvement in the early phase of resuscitation, marked by a continuous flow pattern and normalization of RBCV in the intestinal villi.

It should be noted that these microcirculatory alterations could be characterized only by means of a novel method of data analysis. Similar to other organs, such as the pancreas, brain and skeletal muscle (Borgstrom 1992, Hudetz 1992, Vollmar 1994) the deteriorating intestinal macrocirculation was accompanied by periodic fluctuations in capillary blood flow. This occurred not only during the shock state, but also during the later phase of resuscitation, when the gradually decreasing CI was accompanied by a diminished ileal blood flow and a significant increase in plasma ET-1 level. Since this microvascular oscillatory phenomenon was not observed under control conditions, its appearance can be regarded as a manifestation of tissue malperfusion at any later stage of the experiments. Thus, it appears that the beneficial effect of fluid resuscitation is related not only to the temporary restoration of near-normal microcirculatory velocity values, but also to the re-established continuous flow conditions. Accordingly, the increased length of high-flow phases during flowmotion also reflects improved tissue perfusion. The duration of distinct flow periods is therefore a critical factor and should be taken into account in the data analysis and interpretation. These considerations led us to seek a new method with which to quantify the average microcirculatory flow and its fluctuations, which simultaneously takes into account the changes in both amplitude and duration. Using a probabilistic approach, the instantaneous velocity was regarded as a random variable and the duration for which a particular value of the velocity was observed was used to calculate the probabilities as the relative duration of the high and low oscillatory flow periods. Detailed data analysis demonstrated that the average RBCV decreased and its coefficient of variation increased during HS. More importantly, the analysis revealed that hyperoncotic solution supplemented with an ET-A receptor antagonist

exerted its beneficial effect by maintaining continuous flow in the villi and prolonging the length of high-flow periods at the onset of resuscitation.

The cause of flowmotion is unclear, but a new balance between vasoconstrictor and vasodilator forces can be presumed behind this phenomenon. Flow oscillations could improve the efficacy of tissue oxygenation during low-flow conditions (Tsai 1993). HS is characterized by an intense neuroendocrine response and stress hormone release (Lilly 1986). Norepinephrine induces periodic, intracellular Ca^{2+} -mediated changes in the membrane potential of vascular smooth muscle cells *in vitro* (Gustafsson 1994), and increases flow oscillations in the brain (Hudetz 1992). Therefore, it is conceivable that endogenous catecholamines contribute to local flow pattern regulation. Further, it has been shown that endothelial ET-1 production is enhanced by epinephrine (Kohn 1989). This suggests that the evolving vasoconstriction may be amplified by ET-1 release during HS.

Vasodilator factors are equally important in regulating flowmotion, since vasomotion is dependent on an intact endothelium (Gustafsson 1994). It has been proposed that the interstitial accumulation of vasodilator metabolites leads to precapillary sphincter opening during HS (Dries 1996). A role of CO_2 can be presumed since inhaled CO_2 reversibly abolishes flow oscillations (Hudetz 1992). It is likely, therefore, that arteriolar vasoconstriction is periodically overcome by metabolic or endothelium-derived dilator forces.

The circulating levels of ET-1 were significantly increased during HS and peaked at the end of the observation period. At the onset of resuscitation, significantly higher ET-1 levels could be demonstrated in both HSD-treated groups, with or without ET-A antagonism, than after saline treatment. This is in agreement with the original report, whereby the ET-A receptor inhibitor compound exerted its inhibitory effects directly through specific receptor-binding rather than influencing the circulating levels of endogenous ET-1 (Baranyi 1995). The beneficial effect of ET-A antagonism on the villus microcirculation was also evidenced by the reduced periods of flow cessation. In another study, ET-A receptor antagonism reduced intestinal microvascular injury and PMN leukocyte accumulation during ischemia-reperfusion (Wolfárd 2002, Bajory 2002). The microcirculatory effects of endogenous ET can be linked to a Ca^{2+} -dependent signal transduction mechanism. ET-1 causes sustained oscillatory elevations in intracellular Ca^{2+} level *in vitro*, which could be prevented by ET-A receptor antagonism *in vivo* (Guibert 1999). Thus, the ET-induced Ca^{2+} -mediated catecholamine release could modify microcirculatory responses through an ET-A receptor-dependent mechanism (Hinojosa-Laborde 1993).

In summary, in the presence of time-dependent varying factors, we determined the microcirculatory improvement after hyperoncotic resuscitation and quantitatively compared the microvascular flow-related alterations due to ET-A receptor inhibition.

6. Summary of new findings

- I. HSD-induced positive inotropy and CO elevation is accompanied by ET-1 overproduction and a potentially unfavorable cardiac NO-ET-1 balance. Peripheral NO and ET-1 release could significantly modulate the cardiac contractility through myocardial ET-A receptor activation; the ET-A receptor antagonist pretreatment could reduce the late side-effects of HSD infusion (*i.e.* inhibition of NOS activity) without hemodynamic disadvantages.
- II. As far as we are aware, this is the first *in vivo* evidence of positive inotropy caused by ET-1 following NOS inhibition. A diminished NO production leads to concomitant ET-1 overproduction in the normal myocardium. A reduced NO synthesis leads to a preponderant ET-1 effect, which decreases CO and increases myocardial contractility through an ET-A receptor-dependent mechanism.
- III. Small volume resuscitation with HSD efficiently improves the peripheral tissue microperfusion after experimental HS. ET-A receptor antagonist treatment has favorable microcirculatory consequences in the intestine by increasing the relative duration of high-flow periods in the ileal mucosal villi in the early phase of resuscitation.

7. Acknowledgments

I am grateful to Professors Sándor Nagy and Mihály Boros for the opportunity to work in the Institute of Surgical Research and for their valuable scientific guidance and help. I am indebted to Dr. József Kaszaki, who helped me greatly to learn the necessary surgical and experimental skills. I wish to express my gratitude to Dr. Andrea Szabó who helped me in the critical moments. Special thanks are due to all the technical staff of the Institute. Their skilful activities and enthusiastic work have helped me overcome many difficulties and have greatly facilitated the experiments.

I also thank Dr. Gábor Bogáts and all of my colleagues for their contributions to my experimental work.

Dr. László Németh played a prominent role in my experimental work.

Particular thanks are due to My Wife, My Parents and my whole family, who ensured an appropriate background for me to prepare this work.

8. References

1. Agui T, Xin X, Cai Y, et al.: Stimulation of interleukin-6 production by endothelin in rat bone marrow-derived stromal cells. *Blood* 84:2531-2538, 1994.
2. Anrep GV, V Saalfeld E: The effect of the cardiac contraction upon the coronary flow. *J Physiol* 79:317-331, 1933.
3. Arai H, Hori S, Aramori I, et al.: Cloning and expression of a cDNA encoding an endothelin receptor. *Nature* 348 (6303):730-732, 1990.
4. Armistead CW Jr, Vincent JL, Preiser JC, et al.: Hypertonic saline solution-hetastarch for fluid resuscitation in experimental septic shock. *Anesth Analg* 69:714-720, 1989.
5. Bajory Z, Hutter J, Krombach F, Messmer K: The role of endothelin-1 in ischemia-reperfusion induced acute inflammation of the bladder in rats. *J Urol* 168: 1222-1225, 2002.
6. Banting JD, Friberg P, Adams MA: Acute hypertension after nitric oxide synthase inhibition is mediated primarily by increased endothelin vasoconstriction. *J Hypertens* 14:975-981, 1997.
7. Baranyi L, Campbell W, Ohshima K, et al.: The antisense homology box: a new motif within proteins that encodes biologically active peptides. *Nat Med* 1:894-901, 1995.
8. Baranyi L, Campbell W, Oshima K, et al.: Antisense homology box-derived peptides represent a new class of endothelin receptor inhibitors. *Peptides* 19:211-223, 1998.

9. Battistini B, Forget M-A, Laight D: Potential roles for endothelins in systemic inflammatory response syndrome with a particular relationship to cytokines. *Shock* 5:167-183, 1996.
10. Bergentz S-E: Dextran in the prophylaxis of pulmonary embolism. *World Journal of Surgery* 2:19-25, 1978.
11. Beyer ME, Slezak G, Hoffmeister HM: Significance of Endothelin B receptors for myocardial contractility and myocardial energy metabolism. *J Pharmacol Exp Ther* 278:1228-1234, 1996.
12. Bickell WH, Stern S: Fluid replacement for hypotensive injury victims: how, when and what risks? *Curr Opin Anaesthesiol* 11:177-180, 1998.
13. Blalock JE, Smith EM: Hydropathic anti-complementarity of amino acids based on the genetic code. *Biochem Biophys Res Commun* 121(1):203-207, 1984.
14. Bodin P, Milner P, Marshall J, Burnstock G: Cytokines suppress the shear stress-stimulated release of vasoactive peptides from human endothelial cells. *Peptides* 16:1433-1438, 1995.
15. Boldt J, Knothe C, Zickmann B, et al.: Volume loading with hypertonic saline solution: endocrinologic and circulatory responses. *J Cardiothorac Vasc Anesth* 8:317-323, 1994.
16. Boldt J, Suttner S: Plasma substitutes. *Minerva Anesthesiol* 71:741-758, 2005.
17. Borbely A, Toth A, Edes I, et al.: Peroxynitrite-induced alpha-actinin nitration and contractile alterations in isolated human myocardial cells. *Cardiovasc Res* 67:225-233, 2005.
18. Borgstrom P, Schmidt JA, Bruttig SP, et al.: Slow-wave flowmotion in rabbit skeletal muscle after acute fixed-volume hemorrhage. *Circ Shock* 36:57-61, 1992.
19. Boros M, Massberg S, Baranyi L, et al.: Endothelin 1 induces leucocyte adhesion in submucosal venules of the rat small intestine. *Gastroenterology* 114:103 - 114, 1998.
20. Boulanger C, Luscher TF: Release of endothelin from the porcine aorta. Inhibition by endothelium-derived nitric oxide. *J Clin Invest* 85:587-590, 2002.
21. Casadei B, Sears CE: Nitric-oxide-mediated regulation of cardiac contractility and stretch responses. *Prog Biophys Mol Biol* 82:67-80, 2003.
22. Cassuto J, Cedgard S, Haglund U, et al.: Intramural blood flows and flow distribution in the feline small intestine during arterial hypotension. *Acta Physiol Scand* 106:335-342, 1979.
23. Chang H, Wu GJ, Wang SM, Hung CR: Plasma endothelin level changes during hemorrhagic shock. *J Trauma* 35:825-833, 1993.

24. Clozel M, Gray GA, Breu V, et al.: The endothelin ET-B receptor mediates both vasodilation and vasoconstriction in vivo. *Biochem Biophys Res Commun* 186:867-873, 1992.
25. Davies PF, Robotewskyj A, Griem ML, et al.: Hemodynamic forces and vascular cell communication in arteries. *Arch Pathol Lab Med* 116:1301-1306, 1992.
26. Davies PF, Tripathi S: Mechanical stress mechanism and the cell: an endothelial paradigm. *Circ Res* 72:239-245, 1993.
27. Davies PF: Endothelium as a signal transduction interface for flow forces: cell surface dynamics. *Thrombosis and haemostasis* 70:1-5, 1993.
28. Deitch EA: The role of intestinal barrier failure and bacterial translocation in the development of systemic infection and multiple organ failure. *Arch Surg* 125(3):403-404, 1990.
29. Dries DJ: Hypotensive resuscitation. *Shock* 6:311-316, 1996.
30. Dvorak AM: Mast cell degranulation in human hearts. *N Engl J Med* 315:969, 1986.
31. Ehrenreich H, Anderson RW, Fox CH, et al.: Endothelins, peptides with potent vasoactive properties, are produced by human macrophages. *J Exp Med* 172(6):1741-1748, 1990.
32. Espinosa G, López Farré A, Cernadas MR, et al.: Role of endothelin in the pathophysiology of renal ischemia-reperfusion in normal rabbits. *Kidney Int* 50(3):776-782, 1996.
33. Faist E, Baue AE, Dittmer H, Heberer G: Multiple organ failure in polytrauma patients. *J Trauma* 23(9):775-787, 1983.
34. Feigl EO: Coronary physiology. *Physiol Rev* 63:1-205, 1983.
35. Filep JG: Endogenous endothelin modulates blood pressure, plasma volume, and albumin escape after systemic nitric oxide blockade. *Hypertension* 30:22-28, 1997.
36. Fissthaler B, Dimmeler S, Hermann C, et al.: Phosphorylation and activation of the endothelial nitric oxide synthase by fluid shear stress. *Acta Physiol Scand* 168:81-88, 2000.
37. Frohlich ED: Prolonged local and systemic haemodynamic effects of hyperosmotic solutions. *Arch Int Pharmacodyn* 161:154-166, 1966.
38. Fukunaga M, Fujiwara Y, Ochi S, et al.: Stimulatory effect of thrombin on endothelin-1 production in isolated glomeruli and cultured mesangial cells of rats. *J Cardiovasc Pharmacol* 7:S411-S413, 1991.

39. Fukunaga M, Ochi S, Takama T, et al.: Endothelin-1 stimulates prostaglandin E2 production in an extracellular calcium-independent manner in cultured rat mesangial cells. *Am J Hypertens* 4:137-143, 1991.
40. Fukuroda T, Fujikawa T, Ozaki S, et al.: Clearance of circulating endothelin-1 by ETB receptors in rats. *Biochem Biophys Res Commun* 199:1461-1465, 1994.
41. Galli SJ: New concepts about the mast cell. *New Engl J Med* 328:257-265, 1993.
42. Gardiner SM, Kemp PA, March JE, Bennett T: Effects of bosentan (Ro 47-0203), an ETA-, ETB-receptor antagonist, on regional haemodynamic responses to endothelins in conscious rats. *Br J Pharmacol* 112:823-830, 1994.
43. Goldfarb RD, Lee KJ, Andrejuk T, Dziuban SW Jr.: End-systolic elastance as an evaluation of myocardial function in shock. *Circ Shock* 30:15-26, 1990.
44. Goldfarb RD: Cardiac mechanical performance in circulatory shock: A critical review of methods and results. *Circ Shock* 9:633-653, 1982.
45. Gonzalez-Castillo C, Rubio R, Zenteno-Savin T: Coronary flow-induced inotropism is modulated by binding of dextrans to the endothelial luminal surface. *Am J Physiol Heart Circ Physiol* 284:H1348-1357, 2003.
46. Gregg DE: Effect of coronary perfusion pressure or coronary flow on oxygen usage of the myocardium. *Circ Res* 13:497-500, 1963.
47. Grocott MP, Mythen MG, Gan TJ: Perioperative fluid management and clinical outcomes in adults. *Anesth Analg* 100:1093-1106, 2005.
48. Groner W, Winkelman JW, Harris AG, et al.: Orthogonal polarization spectral imaging: a new method for study of the microcirculation. *Nat Med* 5:1209-1212, 1999.
49. Guibert C, Beech DJ: Positive and negative coupling of the endothelin ETA receptor to Ca^{2+} -permeable channels in rabbit cerebral cortex arterioles. *J Physiol* 514:843-856, 1999.
50. Gustafsson H, Nilsson H: Rhythmic contractions of isolated pressurized small arteries from rat. *Acta Physiol Scand* 152:145-152, 1994.
51. Hahn AW, Resink TJ, Scott-Burden T, et al.: Stimulation of endothelin mRNA and secretion in rat vascular smooth muscle cells: a novel autocrine function. *Cell Regul* 1:649-659, 1990.
52. Hecker M, M Isch A, Bassenge E, Busse R: Vasoconstriction and increased blood flow: two principal mechanisms of shear stress-dependent endothelial autacoid release. *Am J Physiol* 265:H828-H833, 1993.
53. Hinojosa-Laborde C, Lange DL: Endothelin regulation of adrenal function. *Clin Exp Pharmacol Physiol* 26:995-999, 1999.

54. Hudetz AG, Roman RJ, Harder DR: Spontaneous flow oscillations in the cerebral cortex during acute changes in mean arterial pressure. *J Cereb Blood Flow Metab* 12:491-499, 1992.
55. Ihara M, Ishikawa K, Fukuroda T, et al.: In vitro biological profile of a highly potent novel endothelin (ET) antagonist BQ-123 selective for the ETA receptor. *J Cardiovasc Pharmacol* 12:S11-S14, 1992.
56. Imai T, Hirata Y, Emori T, et al.: Induction of endothelin-1 gene by angiotensin and vasopressin in endothelial cells. *Hypertension* 19:753-757, 1992.
57. Ince C: The microcirculation is the motor of sepsis. *Critical Care* 9:S13-S19, 2005.
58. Ishikawa S, Tsukada H, Yuasa H, et al.: Effects of endothelin-1 and conversion of big endothelin-1 in the isolated perfused rabbit lung. *J Appl Physiol* 72:2387-2392, 1992.
59. Ito H, Hirata Y, Adachi S, et al.: Endothelin-1 is an autocrine/paracrine factor in the mechanism of angiotensin II-induced hypertrophy in cultured rat cardiomyocytes. *J Clin Invest* 92:398-403, 1993.
60. Janicki JS, Brower GL, Gardner JD, et al.: Cardiac mast cell regulation of matrix metalloproteinase-related ventricular remodeling in chronic pressure or volume overload. *Cardiovasc Res* 69:657-665, 2006.
61. Karaki H, Sudjarwo SA, Hori M, et al.: ETB receptor antagonist, IRL 1038, selectively inhibits the endothelin-induced endothelium-dependent vascular relaxation. *Eur J Pharmacol* 231:371-374, 1993.
62. Kaszaki J, Wolfard A, Bari F, et al.: Effect of nitric oxide synthase inhibition on myocardial contractility in anesthetized normal and endotoxemic dogs. *Shock* 6:279-285, 1996.
63. Kaszaki J, Wolfárd A, Boros M, et al.: Effects of antiendothelin treatment on the early hemodynamic changes in hyperdynamic endotoxemia. *Acta Chirurg Hung* 36:152-153, 1997.
64. Kinnunen P, Szokodi I, Nicholls MG, Ruskoaho H: Impact of NO on ET-1- and AM-induced inotropic responses: potentiation by combined administration. *Am J Physiol Regul Integr Comp Physiol* 279:R569-R575, 1997.
65. Kohno M, Murakawa K, Yokokawa K, et al.: Production of endothelin by cultured porcine endothelial cells: modulation by adrenaline. *J Hypertens* 7:S130-S131, 1989.
66. Konrad D, Oldner A, Wanecek M, et al.: Positive inotropic and negative lusitropic effects of endothelin receptor agonism in vivo. *Am J Physiol* 289:H1702-H1709, 2005.

67. Kourembanas S, McQuillan LP, Leung GK, Faller DV: Nitric oxide regulates the expression of vasoconstrictors and growth factors by vascular endothelium under both normoxia and hypoxia. *J Clin Invest* 92:99-104, 1993.
68. Kramer GC, Perron PR, Lindsey DC: Small-volume resuscitation with hypertonic saline dextran solution. *Surgery* 100:239-246, 1986.
69. Kuchan MJ, Frangos JA: Shear stress regulates endothelin-1 release via protein kinase C and cGMP in cultured endothelial cells. *Am J Physiol* 264:H150-H156, 1993.
70. Kuebler WM, Abels C, Schuerer L, Goetz AE: Measurement of neutrophil content in brain and lung tissue by a modified myeloperoxidase assay. *Int J Microcirc Clin Exp* 16:89-97, 1996.
71. Lilly MP, Engeland WC, Gann DS: Adrenal medullary responses to repeated hemorrhage in conscious dogs. *Am J Physiol* 251:R1193-R1199, 1986.
72. Macarthur H, Warner TD, Wood EG, et al.: Endothelin-1 release from endothelial cells in culture is elevated both acutely and chronically by short periods of mechanical stretch. *Biochem Biophys Res Commun* 200(1):395-400, 1994.
73. Madorin WS, Martin CM, Sibbald WJ: Dopexamine attenuates flow motion in ileal mucosal arterioles in normotensive sepsis. *Crit Care Med* 27:394-400, 1999.
74. Maeda S, Miyauchi T, Iemitsu M, et al.: Endothelin receptor antagonist reverses decreased NO system in the kidney in vivo during exercise. *Am J Physiol Endocrinol Metab* 286:E609-E614, 2004.
75. Malek A, Izumo S: Physiological fluid shear stress causes downregulation of endothelin-1 mRNA in bovine aortic endothelium. *Am J Physiol* 263:C389-C396, 1992.
76. Massion PB, Feron O, Dessy C, Balligand JL: Nitric oxide and cardiac function: ten years after, and continuing. *Circ Res* 93:388-398, 2003.
77. Mazzoni MC, Borgström P, Intaglietta M, Arfors K-E: Capillary narrowing in hemorrhagic shock is rectified by hyperosmotic saline-dextran reinfusion. *Circulatory Shock* 31:407-418, 1990.
78. Menger MD, Thierjung C, Hammersen F, Messmer K: Dextran versus HES in inhibition of post-ischaemic leukocyte adherence in striated muscle. *Circulatory Shock* 41:248, 1993.
79. Menger MD, Thierjung C, Hammersen F, Messmer K: Influence of isovolaemic haemodilution with dextran and HAES on the PMN-endothelium interaction in postischaemic skeletal muscle. *European Surgical Research* 21:74, 1989.

80. Menger MD: Microcirculatory disturbances secondary to ischemia-reperfusion. *Transplant Proc* 27:2863-2865, 1995.
81. Messmer K, Kreimeier U: Microcirculatory therapy in shock. *Resuscitation* 18:S51-S61, 1989.
82. Miller VM, Burnett JC Jr: Modulation of NO and endothelin by chronic increases in blood flow in canine femoral arteries. *Am J Physiol* 263:H103-H108, 1992.
83. Murray DB, Gardner JD, Brower GL, Janichi JS: Endothelin-1 mediates cardiac mast cell degranulation, matrix metalloproteinase activation and myocardial remodeling in rats. *Am J Physiol* 287:H2405-H2409, 2004.
84. Neylon CB: Vascular biology of endothelin signal trasduction. *Clin Exp Pharmacol* 26:149-153, 1999.
85. Nolte D, Lehr H-A, Messmer K: Dextran and adenosine-coupled dextran reduce post-ischaemic leukocyte adherence in postcapillary venules of the hamster. *Progress in Applied Microcirculation* 18:103, 1991.
86. Ohnishi M, Wada A, Tsutamoto T, et al.: Endothelin stimulates an endogenous nitric oxide synthase inhibitor, asymmetric dimethylarginine, in experimental heart failure. *Clin Sci* 103:241S-244S, 2002.
87. Otsuka A, Mikami H, Tsunetoshi T, et al.: Increased plasma level of endothelin with vasoconstriction after dextran infusion. *Biochem Int* 22:353-359, 1990.
88. Ovadia B, Bekker JM, Fitzgerald RK, et al.: Nitric oxide-endothelin-1 interaction after acute ductal constriction in fetal lambs. *Am J Physiol* 282:H862-H871, 2002.
89. Ozaki S, Ohwaki K, Ihara M, et al.: ETB-mediated regulation of extracellular levels of endothelin-1 in cultured human endothelial cells. *Biochem Biophys Res Commun* 209(2):483-489, 1995.
90. Pearson JD: Endothelial cell biology. *Radiology* 179:9-14, 1991.
91. Pohl U, Holtz J, Busse R, Bassenge E: Crucial role of endothelium in the vasodilator response to increased flow in vivo. *Hypertension* 8:37-47, 1986.
92. Prendergast BD, Sagach VF, Shah AM: Basal release of nitric oxide augments the Frank-Starling response in the isolated heart. *Circulation* 96:1320-1329, 1997.
93. Rakugi H, Tabuchi Y, Nakamaru M, et al.: Evidence for endothelin-1 release from resistance vessels of rats in response to hypoxia. *Biochem Biophys Res Commun* 169:973-977, 1990.

94. Richard J, Hogie M, Clozel M, Loffler BM, Thuillez C: In vivo evidence of an endothelin-induced vasopressor tone after inhibition of nitric oxide synthesis in rats. *Circulation* 91:771-775, 1997.
95. Robu VG, Pfeiffer ES, Robia SL, et al.: Localization of functional endothelin receptor signaling complexes in cardiac transverse tubules. *J Biol Chem* 278:48154-48161, 2003.
96. Rutherford RB, Jones DN: Does dextran improve graft patency? *Journal of Vascular Surgery* 1:765, 1988.
97. Sakurai T, Yanagisawa M, Takuwa Y, et al.: Cloning of a cDNA encoding a non-isopeptide-selective subtype of the endothelin receptor. *Nature* 348(6303):732-735, 1990.
98. Scalia S, Burton H, Van Wylen D, et al.: Persistent arteriolar constriction in microcirculation of the terminal ileum following moderate hemorrhagic hypovolemia and volume restoration. *J Trauma* 30(6):713-718, 1990.
99. Scalia S, Sharma P, Rodriguez J, et al.: Decreased mesenteric blood flow in experimental multiple organ failure. *J Surg Res* 52(1):1-5, 1992.
100. Scalia SV, Taheri PA, Force S, et al.: Mesenteric microcirculatory changes in nonlethal hemorrhagic shock: the role of resuscitation with balanced electrolyte or hypertonic saline/dextran. *J Trauma* 33(2):321-315, 1992.
101. Scannell G, Clark L, Waxman K: Regional flow during experimental hemorrhage and crystalloid resuscitation: persistence of low flow to the splanchnic organs. *Resuscitation* 23(3):217-225, 1992.
102. Schlichting E, Aspelin T, Grotmol T, Lyberg T: Endothelin and hemodynamic responses to superior mesenteric artery occlusion shock and hemorrhagic shock in pigs. *Shock* 3:109-115, 1995.
103. Sessa WC, Kaw S, Hecker M, Vane JR: The biosynthesis of endothelin-1 by human polymorphonuclear leukocytes. *Biochem Biophys Res Commun* 174(2):613-618, 1991.
104. Sessa WC, Kaw S, Zembowicz A, et al.: Human polymorphonuclear leukocytes generate and degrade endothelin-1 by two distinct neutral proteases. *J Cardiovasc Pharmacol* 17:S34-S38, 1991.
105. Sheehy AM, Burson MA, Black SM: Nitric oxide exposure inhibits endothelial NOS activity but not gene expression: a role for superoxide. *Am J Physiol* 274:L833-L841, 1998.
106. Shetty SS, Okada T, Webb RL, et al.: Functionally distinct endothelin-B receptors in vascular endothelium and smooth muscle. *Biochem Biophys Res Commun* 191:459-467, 1993.

107. Sumner MJ, Cannon TR, Mundin JW, et al.: Endothelin ETA and ETB receptors mediate vascular smooth muscle contraction. *Br J Pharmacol* 107: 858-860, 1992.
108. Szabó A, Suki B, Csonka E, et al.: Flow motion in the intestinal villi during hemorrhagic shock: a new method to characterize the microcirculatory changes. *Shock* 21:320-328, 2004.
109. Szabó C, Mitchell JA, Thiernemann C, Vane JR: Nitric oxide-mediated hyporeactivity to noradrenaline precedes the induction of nitric oxide synthase in endotoxin shock. *Br J Pharmacol* 108:786-792, 1993.
110. Tanaka T, Tsukuda E, Nozawa M, et al.: RES-701-1, a novel, potent, endothelin type B receptor-selective antagonist of microbial origin. *Mol Pharmacol* 45(4):724-730, 1994.
111. Theuer CJ, Wilson MA, Steeb GD, et al.: Microvascular vasoconstriction and mucosal hypoperfusion of the rat small intestine during bacteremia. *Circ Shock* 40:61-68, 1993.
112. Tsai AG, Friesenecker B, Intaglietta M: Capillary flow impairment and functional capillary density. *Int J Microcirc Clin Exp* 15:238-243, 1995.
113. Tsai AG, Intaglietta M: Evidence of flowmotion induced changes in local tissue oxygenation. *Int J Microcirc Clin Exp* 12:75-88, 1993.
114. Turner AJ, Tanzawa K: Mammalian membrane metallopeptidases: NEP, ECE, KELL, and PEX. *FASEB J* 11(5):355-364, 1997.
115. Uchida Y, Jun T, Ninomiya H, et al.: Involvement of endothelins in immediate and late asthmatic responses of guinea pigs. *J Pharmacol Exp Ther* 277(3):1622-1629, 1996.
116. Vallet B, Lund N, Curtis SE, et al.: Gut and muscle tissue PO₂ in endotoxemic dogs during shock and resuscitation. *J Appl Physiol* 76:793-800, 1994.
117. Vallet B: Endothelial cell dysfunction and abnormal tissue perfusion. *Crit Care Med* 30:S229-S234, 2002.
118. van Wamel AJ, Ruwhof C, van der Valk-Kokshoom LE, et al.: The role of angiotensin II, endothelin-1 and transforming growth factor-beta as autocrine/paracrine mediators of stretch-induced cardiomyocyte hypertrophy. *Mol Cell Biochem* 218:113-124, 2001.
119. Velasco IT, Pontieri V, Rocha e Silva M, Lopes OU: Hyperosmotic NaCl and severe hemorrhagic shock. *Am J Physiol* 239:H664-H673, 1980.
120. Verhaar MC, Strachan FE, Newby DE, et al.: Endothelin-A receptor antagonist-mediated vasodilatation is attenuated by inhibition of nitric oxide synthesis and by endothelin-B receptor blockade. *Circulation* 97:752 -756, 1998.
121. Vollmar B, Menger MD: Volume replacement and microhemodynamic changes in polytrauma. *Langenbecks Arch Surg* 389(6):485-491, 2004.

122. Vollmar B, Preissler G, Menger MD: Hemorrhagic hypotension induces arteriolar vasomotion and intermittent capillary perfusion in rat pancreas. *Am J Physiol* 267:H1936-H1940, 1994.
123. Wang P, Hauptman JG, Chaudry IH: Hemorrhage produces depression in microvascular blood flow which persists despite fluid resuscitation. *Circ Shock* 32(4):307-318, 1990.
124. Warner TD: Relationships between the endothelin and nitric oxide pathways. *Clin Exp Pharmacol Physiol* 26:247-252, 1999.
125. Wesson DE, Simoni J, Green DF: Reduced extracellular pH increases endothelin-1 secretion by human renal microvascular endothelial cells. *J Clin Invest* 101:578-583, 1998.
126. Wolfárd A, Szalay L, Kaszaki J, et al.: Dynamic in vivo observation of villus microcirculation during small bowel autotransplantation: effects of endothelin-A receptor inhibition. *Transplantation* 73:1511-1514, 2002.
127. Yamamura H, Nabe T, Kohno S, Ohata K: Endothelin-1, one of the most potent histamine releasers in mouse peritoneal cells. *Eur J Pharmacol* 265:9-15, 1994.
128. Yanagisawa M, Kurihara H, Kimura S, et al.: A novel potent vasoconstrictor peptide produced by vascular endothelial cells. *Nature* 332:411-415, 1988.

ANNEX

- I. **Eszlári E**, Czóbel M, Molnár G, Bogáts G, Kaszaki J, Nagy S, Boros M: Modulation of cardiac contractility through endothelin-1 release and myocardial mast cell degranulation. *Acta Physiol Hun* 95:301-319, 2008.
- II. Molnár G, **Eszlári E**, Czóbel M, Kaszaki J, Bogáts G, Nagy S, Boros M: A nitrogén-monoxid-szintézis gátlása endothelinfüggő szívkontraktilitás növekedéshez vezet. *Cardiologica Hungarica* 40(1):1-6, 2010.
- III. Szabó A, Suki B, Csonka E, **Eszlári E**, Kucska K, Vajda K, Kaszaki J, Boros M: Flowmotion in the intestinal villi during hemorrhagic shock. A new method to characterize the microcirculatory changes. *Shock* 21:320-329, 2004.